

Heteroleptic Organostannylenes and an Organoplumbylene Bearing Phosphorus-Containing Pincer-Type Ligands – Structural Variations and Insights into the Configurational Stability

Markus Henn,^[a] Vajk Deák,^[a] Stefan Krabbe,^[a] Markus Schürmann,^[a] Marc H. Prosenc,^[b] Sonja Herres-Pawlits,^[a] Bernard Mahieu,^[c] and Klaus Jurkschat^{*[a]}

In Memory of Professor Herbert Schumann

Keywords: Organostannylenes; Organoplumbbylenes; Density functional calculations; Arylphosphonic esters; Pincer-type ligands

Abstract. The syntheses of the arylphosphonic esters 3-Br-5-*t*Bu-1-{P(O)(O*i*Pr)₂}C₆H₃ (**1**), 5-*t*Bu-1,3-{P(O)(O*i*Pr)₂}₂C₆H₃ (**2**), of the heteroleptic intramolecularly coordinated organostannylenes [4-*t*Bu-2,6-{P(O)(O*i*Pr)₂}₂C₆H₂]SnX (**3**, X = Cl; **4**, X = Br; **5**, X = I; **6**, X = SPh), the organoplumbylene [4-*t*Bu-2,6-{P(O)(O*i*Pr)₂}₂C₆H₂]PbCl (**7**), and the transition metal complex [4-*t*Bu-2,6-{P(O)(O*i*Pr)₂}₂C₆H₂]Sn(Cl)-Cr(CO)₅ (**8**) are reported. The compounds were characterized by ¹H, ¹³C, ³¹P, ³¹P MAS (**3**), ¹¹⁹Sn, and ¹¹⁹Sn MAS (**3**) NMR spectroscopy, electrospray ionization mass spectrometry (**3**), Mössbauer spectroscopy (**3–5, 8**) and single-crystal X-ray diffraction analyses (**2, 3–5, 6–8**). In contrast to its ethoxy-substituted analogue [4-*t*Bu-2,6-{P(O)(OEt)₂}₂C₆H₂]SnCl, compound **3**, like the thiophenolate derivative **6**, is monomeric in solution as well as in the solid state. This difference is also manifested by the Mössbauer as well as solid state NMR spectroscopic data. On the other hand, the corresponding organoplumbylene **7** shows a similar chlorido-bridged polymeric structure as its ethoxy-

substituted analogue. Variable-temperature and concentration-dependent ¹H and ³¹P NMR spectra reveal, on the respective time scales, the tin atom in compound **3** to be configurationally unstable and those in compounds **6** and **8** to be configurationally stable. DFT calculations support a chlorido-bridged dimer to account for the configurational instability in compound **3**. Surprisingly and in contrast to compounds **3** and **6**, the organobromido- and organoiodidostannylenes **4** and **5**, respectively, show intermolecular Sn···Sn distances of 3.6809(4) and 3.5953(4) Å being shorter than twice the van der Waals radius of tin (2.20 Å). Quantum chemical calculations were performed on monomeric and dimeric model compounds, which revealed a weak Sn···Sn bonding interaction for dimer **3** (16 kJ·mol⁻¹) as well as for dimer **5** (20 kJ·mol⁻¹) whereas the hypothetical model compound *p*-*t*BuC₆H₄SnI showed an iodido-bridged dimer rather than a Sn···Sn bonding interaction.

Introduction

Among the class of low-valent tin compounds heteroleptic organostannylenes of type *R*SnX (*R* = organic substituent with or without donor functionality, X = F, Cl, Br, I, N(SiMe₃)₂, SC(S)C₆H₂-*t*Bu₃-2,4,6, Si(SiMe₃)₃, Sn(SiMe₃)₃) have attracted increasing interest over the last two decades.^[1] Compounds of this type are used for the synthesis of novel unsymmetrically substituted diorganostannylenes of type *RR'*Sn^[1b,s] as well as

of organotin(IV) compounds of type *RR'SnXY* (*R'* = organic substituent; Y = halogen).^[2] Moreover, they are precursors for the syntheses of organotin(I) compounds, *R*SnSn*R*,^[3] the formal tin analogues of alkynes, and of compounds such as *R*SnW(PR₃)₄Cl^[4] and *R*Sn*M*(Cp)(CO)₃ (*M* = Cr, Mo, W)^[5] with the former containing a formal tin–transition metal triple bond. Only recently, *R*SnX-type compounds (X = Cl, H) have been employed, in combination with SnCl₂, for the synthesis of the spectacular heptanuclear organotin cluster [Sn₇{C₆H₃-2,6-(C₆H₃-2,6-*i*Pr₂)₂}]^[6].

Heteroleptic organotin(II) halides, *R*SnX (X = Cl, Br, I), with the *R* group containing an intramolecularly coordinating donor function are usually monomeric both in solution and in the solid state with the exception of [Sn{C₆H₃(NMe₂)₂-2,6}Cl]^[7] and [Sn{CH(SiMe₃)C₉H₆N-8}Br]^[8] each showing head-to-tail dimerization via intermolecular N→Sn (3.204(4) Å) and Br→Sn (3.420 Å) coordination, respectively. For those *R*SnCl type compounds containing bulky substituents *R* monomers as well as dimers (via intermolecular Sn–Cl···Sn bridges) were reported for the solid state, to the extent that for [2,6-{2,4,6-(*i*Pr)₃C₆H₂}₂C₆H₃]SnCl both monomer and dimer coexist in one

* Prof. Dr. K. Jurkschat
Fax: +49-231-7555048

E-Mail: klaus.jurkschat@tu-dortmund.de

[a] Lehrstuhl für Anorganische Chemie II
Technische Universität Dortmund
Otto-Hahn-Str. 6
44227 Dortmund, Germany

[b] Institut für Anorganische und Angewandte Chemie
Universität Hamburg
20146 Hamburg, Germany

[c] Laboratoire de Chimie Structurale (CSTR)
Université de Louvain
1348 Louvain-la-Neuve, Belgium

Supporting information for this article is available on the WWW under <http://dx.doi.org/10.1002/zaac.201000387> or from the author.

unit cell.^[1p] Notably, among the crystallographically characterized heteroleptic organotin(II) halides $RSnX$ there are only two examples with $X = Br^{[8,9]}$ and two examples with $X = I^{[11,p]}$ respectively.

The 1H NMR spectra of both $(2,6-Me_2NCH_2)_2C_6H_3SnCl^{[1b]}$, $\sigma-C_5H_4NC(SiMe_3)_2SnX$ ($X = Cl, N(SiMe_3)_2^{[1d]}$) and $8-C_9H_6NCH(SiMe_3)SnX$ ($X = Cl, Br^{[8]}$) were reported to be temperature-dependent. For the former compound, at $-70\text{ }^\circ C$, both the methylene and methyl protons are diastereotopic and indicate the lone pair at the tin atom to be stereochemically active. Coalescence phenomena of the CH_2 and NMe_2 proton resonances above $-65\text{ }^\circ C$ were interpreted in terms of intramolecular rearrangement processes such as $Sn-N$ dissociation/association and inversion of configuration at the tin atom. However, no attempts were made to distinguish between these two alternatives.^[1b] Later on and based on a more detailed study including concentration dependence of coalescence temperatures, however, inversion of configuration at the tin atom was favored.^[10] Nevertheless, for the two latter compounds, the coalescence phenomena observed for the methyl proton resonances were discussed in terms of combined $N \rightarrow Sn$ bond dissociation and rotation about the $Sn-C$ bond.^[1d,8]

For some years we have been interested in the application of phosphorus-containing O,C,O-coordinating pincer-type ligands to the synthesis of a variety of organoelement compounds.^[11] In course of these studies we also prepared the heteroleptic organostannylene $[4-tBu-2,6-\{P(O)(OEt)_2\}_2C_6H_2]SnCl$ and noticed a considerable difference of the ^{119}Sn NMR chemical shifts in solution ($\delta = -100$) and in the solid state ($\delta = -160$).^[10] Moreover, addition of $[(Ph_3P)_2N]^+Cl^-$ to a solution of $[4-tBu-2,6-\{P(O)(OEt)_2\}_2C_6H_2]SnCl$ in CD_2Cl_2 caused low-frequency shift of the ^{119}Sn resonance to $\delta = -163$, a value being close to that of the chemical shift in the solid state.^[10] The results were interpreted in terms of $[4-tBu-2,6-\{P(O)(OEt)_2\}_2C_6H_2]SnCl$ being monomeric in solution but, via chlorido bridges, dimeric (or oligomeric) in the solid state, like the corresponding organoplumbylene $[4-tBu-2,6-\{P(O)(OEt)_2\}_2C_6H_2]PbCl$.^[11g] Unfortunately, no single crystals of $[4-tBu-2,6-\{P(O)(OEt)_2\}_2C_6H_2]SnCl$ suitable for X-ray diffraction analysis could be obtained to verify this interpretation.

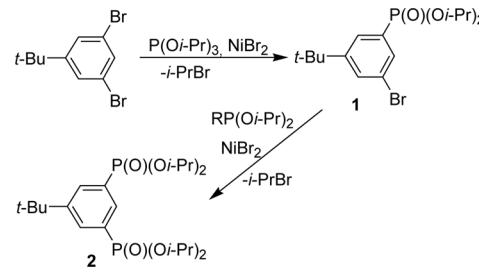
Bearing in mind the superior crystallization properties of organoelement compounds containing the isopropoxy- instead of the ethoxy-substituted pincer-type ligand we decided to synthesize $[4-tBu-2,6-\{P(O)(O*i*Pr)₂\}_2C_6H_2]Sn(L)X$ ($X = Cl, Br, I; L =$ lone pair, $Cr(CO)_5$) and to study their structures in solution as well as in the solid state. We also prepared $[4-tBu-2,6-\{P(O)(O*i*Pr)₂\}_2C_6H_2]SnSPh$ which is, to the best of our knowledge, the first structurally characterized organotin(II) thiolate. We learned that the structures of these compounds in the solid state depend indeed on the identity of the substituents at the phosphorus atom as well as on the X atom even though the former are remote from the tin atom. Moreover, we found that the configurational stability in solution of the tin atom in intramolecularly coordinated heteroleptic organostannyles of type $RSn(L)X$ depends on the identity of X and L . For the sake of comparison, the molecular structures of the protonated ligand $5-tBu-1,3-\{P(O)(O*i*Pr)₂\}_2C_6H_3$ and of the heteroleptic

organoplumbylene $[4-tBu-2,6-\{P(O)(O*i*Pr)₂\}_2C_6H_2]PbCl$ were also determined. Notably, in the latter, the isopropoxy substituents at the phosphorus atoms do not change the solid-state structure as compared to the ethoxy-substituted analogue.

Results and Discussion

Syntheses and Molecular Structures in the Solid State

The $NiBr_2$ -catalyzed reaction of triisopropyl phosphite, $P(O*i*Pr)₃$, with the aryl dibromide $1,3-Br_2-5-tBuC_6H_3$ gave, depending on the stoichiometry of the reagents, the arylphosphonic ester $3-Br-5-tBu-1-\{P(O)(O*i*Pr)₂\}C_6H_3$ (**1**) and the arylidiphosphonic ester $5-tBu-1,3-\{P(O)(O*i*Pr)₂\}_2C_6H_3$ (**2**) in good yields (Scheme 1). Compound **1** is a colorless oil whereas compound **2** is a colorless crystalline material.



Scheme 1. Synthesis of compounds **1** and **2**.

The molecular structure of compound **2** is shown in Figure 1 together with selected structural parameters.

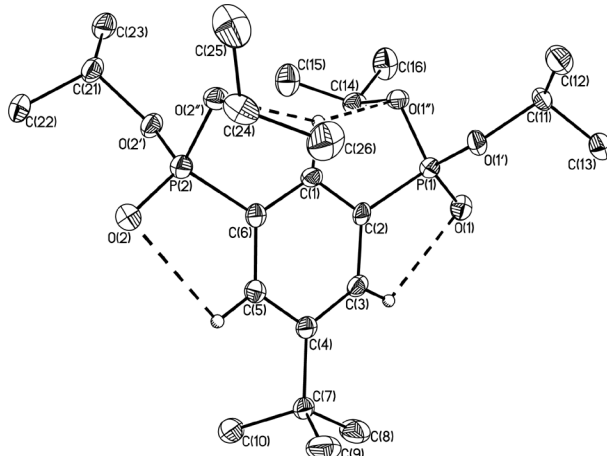
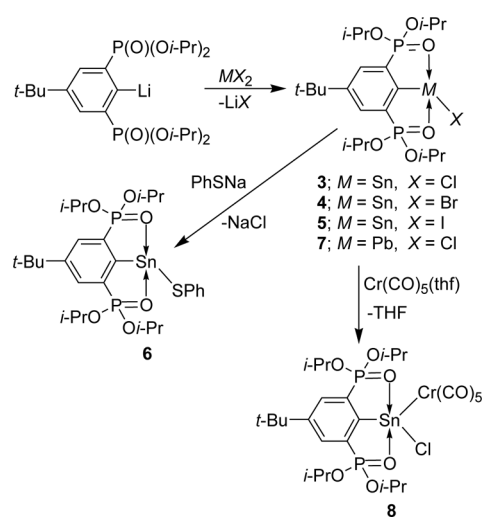


Figure 1. Molecular structure of compound **2**. Selected interatomic distances / \AA : $P(1)-O(1)$ 1.469(3), $P(1)-O(1')$ 1.565(3), $P(1)-O(1'')$ 1.582(3), $P(2)-O(2)$ 1.468(3), $P(2)-O(2')$ 1.570(3), $P(2)-O(2'')$ 1.586(3), $O(1)\cdots H(3)$ 2.65(4), $O(2)\cdots H(5)$ 2.68(4). Selected interatomic angles /deg: $C(1)-C(2)-P(1)$ 120.0(3), $C(1)-C(6)-P(2)$ 120.5(3), $O(1)-P(1)-O(1')$ 117.7(2), $O(1)-P(1)-O(1'')$ 114.6(2), $O(1')-P(1)-O(1'')$ 102.5(2), $O(1)-P(1)-C(2)$ 113.4(2), $O(1')-P(1)-C(2)$ 100.7(2), $O(1')-P(1)-C(2)$ 106.3(2), $O(2)-P(2)-O(2')$ 117.9(2), $O(2)-P(2)-O(2'')$ 114.2(2), $O(2')-P(2)-O(2'')$ 102.1(2), $O(2)-P(2)-C(6)$ 113.2(2), $O(2')-P(2)-C(6)$ 100.3(2), $O(2'')-P(2)-C(6)$ 107.6(2). Selected torsion angles /deg: $O(1)-P(1)-C(2)-C(3)$ 17.6(4), $O(2)-P(2)-C(6)-C(5)$ 11.1(4).

Compound **2** crystallized in the triclinic space group $P\bar{1}$ with two molecules per unit cell.

Like in its ethoxy-substituted analogue $5-t\text{Bu}-1,3-\{\text{P}(\text{O})(\text{OEt})_2\}_2\text{C}_6\text{H}_3$,^[11h] both $\text{P}=\text{O}$ oxygen atoms O(1) and O(2) point away from the hydrogen atom H(1), but in contrast to the latter they are only slightly displaced from the aromatic plane. There are intramolecular $\text{O}(1)\cdots\text{H}(3)$ and $\text{O}(2)\cdots\text{H}(5)$ distances of 2.65(4) and 2.68(4) Å, respectively, that are shorter than the van der Waals distances^[12] of oxygen (1.50 Å) and hydrogen (1.20–1.45 Å). Somewhat longer but still in the range of the sum of the van der Waals radii are the $\text{O}(1')\cdots\text{H}(1)$ and $\text{O}(2')\cdots\text{H}(1)$ distances of 2.70(4) and 2.87(4) Å, respectively. Associated with this are slightly longer $\text{P}(1)-\text{O}(1')$ and $\text{P}(2)-\text{O}(2')$ distances of 1.582(3) and 1.586(3) Å, respectively. It is still a matter of controversial debate^[13] whether or not weak C–H···O interactions in the order of magnitude of 0.5–2.0 kcal·mol⁻¹ influence the molecular structure that is actually observed in the solid state. One has to be aware that these low energy effects can be superimposed by crystal packing forces.

The reaction of the *in situ*-generated organolithium salt [$4-t\text{Bu}-2,6-\{\text{P}(\text{O})(\text{O}i\text{Pr})_2\}_2\text{C}_6\text{H}_2\text{Li}$] with tin(II) halides, SnX_2 , and lead dichloride, PbCl_2 , provided the heteroleptic organostannyles [$4-t\text{Bu}-2,6-\{\text{P}(\text{O})(\text{O}i\text{Pr})_2\}_2\text{C}_6\text{H}_2\text{SnX}_2$] (**3**, $X = \text{Cl}$; **4**, $X = \text{Br}$; **5**, $X = \text{I}$) and the organoplumbylene [$4-t\text{Bu}-2,6-\{\text{P}(\text{O})(\text{O}i\text{Pr})_2\}_2\text{C}_6\text{H}_2\text{PbCl}$] (**7**), respectively, in good yields (Scheme 2). The reaction of the organochloridostannylene **3** with sodium thiophenolate and *in situ*-generated chromiumpentacarbonyl tetrahydrofuranate, $\text{Cr}(\text{CO})_5(\text{thf})$, gave the organotin(II)thiophenolate [$4-t\text{Bu}-2,6-\{\text{P}(\text{O})(\text{O}i\text{Pr})_2\}_2\text{C}_6\text{H}_2\text{SnSPPh}$] (**6**), and the chromiumpentacarbonyl organostannylene complex [$4-t\text{Bu}-2,6-\{\text{P}(\text{O})(\text{O}i\text{Pr})_2\}_2\text{C}_6\text{H}_2\text{Sn}(\text{Cl})\text{Cr}(\text{CO})_5$] (**8**), respectively (Scheme 2). Compounds **3** and **6** are colorless whereas **4**, **5**, **7**, and **8** are yellow and green, respectively, crystalline solids that are well-soluble in common organic solvents such as benzene, THF, and dichloromethane.



Scheme 2. Synthesis of the organostannyles **3–6**, the transition metal complex **8**, and of the organoplumbylene **7**.

The molecular structures of the chlorido-, iodido-, and thiophenolato-substituted compounds **3**, **5** and **6**, respectively, are shown in Figure 2, Figure 3, and Figure 4, and that of the bromido-substituted derivative **4** is depicted in the Supporting In-

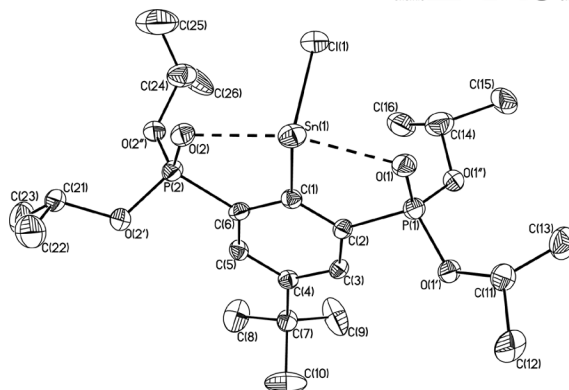


Figure 2. Molecular structure of compound **3**.

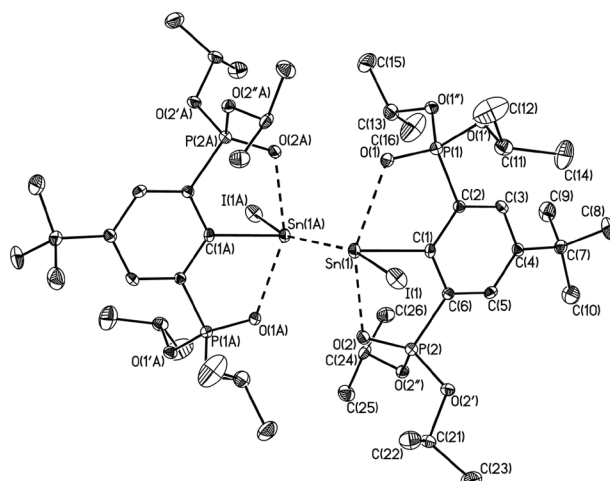


Figure 3. Molecular structure of compound **5**.

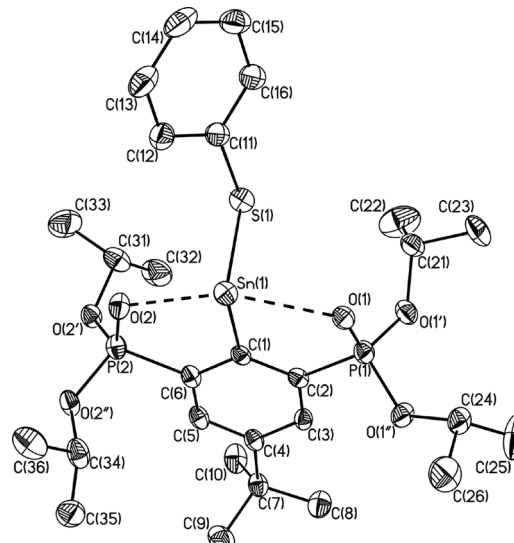


Figure 4. Molecular structure of compound **6**.

Table 1. Selected bond lengths /Å, bond angles, and torsion angles /deg for compounds **3–7**.

	3 ($M = \text{Sn}, X = \text{Cl}$)	4 ($M = \text{Sn}, X = \text{Br}$)	5 ($M = \text{Sn}, X = \text{I}$)	6 ($M = \text{Sn}, X = \text{S}$)	7 ($M = \text{Pb}, X = \text{Cl}$)
$M(1)-\text{C}(1)$	2.244(2)	2.237(2)	2.233(2)	2.231(3)	2.334(4)
$M(1)-X(1)$	2.4708(8)	2.6286(3)	2.8544(3)	2.512(1)	2.836(1)
$M(1)-X(1\text{A})$					2.879(1)
$M(1)-\text{O}(1)$	2.430(2)	2.463(2)	2.473(2)	2.478(2)	2.560(2)
$M(1)-\text{O}(2)$	2.427(2)	2.420(2)	2.408(2)	2.434(2)	
$\text{P}(1)-\text{O}(1)$	1.489(2)	1.484(1)	1.487(2)	1.485(2)	1.485(2)
$\text{P}(2)-\text{O}(2)$	1.483(2)	1.490(2)	1.491(2)	1.485(2)	
$\text{C}(1)-M(1)-X(1)$	94.23(6)	93.73(0)	94.92(6)	89.38(8)	90.5(1)
$\text{O}(1)-M(1)-\text{O}(2)$	152.01(6)	151.94(0)	152.23(6)	152.48(7)	147.1(1)
$\text{C}(1)-\text{C}(2)-\text{P}(1)$	115.8(2)	117.34(16)	116.8(2)	114.9(2)	117.6(2)
$\text{C}(1)-\text{C}(6)-\text{P}(2)$	115.1(2)	115.55(0)	115.5(2)	116.9(3)	
$M(1)-X(1)-\text{C}(11)$				100.4(1)	
$X(1)-M(1)-M(1\text{A})$		170.38(1)	166.96(1)		
$X(1)-M(1)-X(1\text{A})$					176.4(1)
$M(1)-X(1\text{A})-M(1\text{A})$					126.8(1)
$\text{C}(1)-\text{Sn}(1)-\text{Sn}(1\text{A})-\text{C}(1\text{A})$		180.0(1)	180.0(9)		
$X(1)-\text{Sn}(1)-\text{Sn}(1\text{A})-X(1\text{A})$		180.0(1)	180.0(1)		
$M(1)-\text{C}(1)-\text{C}(2)-\text{C}(3)$	175.2(2)	-177.0(1)	174.9(2)	171.2(2)	173.5(2)
$\text{O}(1)-\text{P}(1)-\text{C}(2)-\text{C}(3)$	-174.3(2)	-179.9(1)	179.1(2)	-165.4(3)	-170.0(2)
$\text{O}(2)-\text{P}(2)-\text{C}(6)-\text{C}(5)$	171.9(2)		172.8(2)	174.0(3)	

formation (Figure S1). Selected geometric parameters are collected in Table 1.

Compound **3** crystallizes in the orthorhombic space group $P2_12_12_1$ with four molecules in the unit cell. The compounds **4** and **5** are isostructural and crystallize like compound **6** monoclinically in the space group $P2_1/c$ with four molecules per unit cell as well. Both compounds **3** and **6** are essentially monomeric; the shortest intermolecular $\text{Sn}\cdots\text{Sn}$ and $\text{Sn}\cdots\text{Cl}$ distances of 8.2966(2) and 7.2568(8) Å, respectively, being beyond the sum of the van der Waals radii^[12] of the respective atoms. By contrast, the organobromido- and organoiodidostannylenes **4** and **5**, respectively, reveal intermolecular $\text{Sn}\cdots\text{Sn}$ distances

of 3.6809(4) (**4**) and 3.5953(4) Å (**5**) that are shorter than twice the van der Waals radius of tin (2.20 Å). To the best of our knowledge, this is unprecedented for heteroleptic organostannylene of type $R\text{Sn}X$ ($X = \text{halogen}$) for which $R\text{Sn}-X\cdots\text{Sn}(X)R$ rather than $R(X)\text{Sn}\cdots\text{Sn}(X)R$ bridges are to be expected. Thus, Leung and co-workers reported the structure of intramolecularly coordinated 8-NC₉H₆(Me₃Si)CHSnBr^[8] that forms a head-to-tail dimer through a SnBrSnBr four-membered ring. However, a rather similar $\text{Sn}\cdots\text{Sn}$ distance of 3.639(1) Å was reported for one out of two modifications of $[2,4,6-(\text{CF}_3)_3\text{C}_6\text{H}_2]_2\text{Sn}$.^[14]

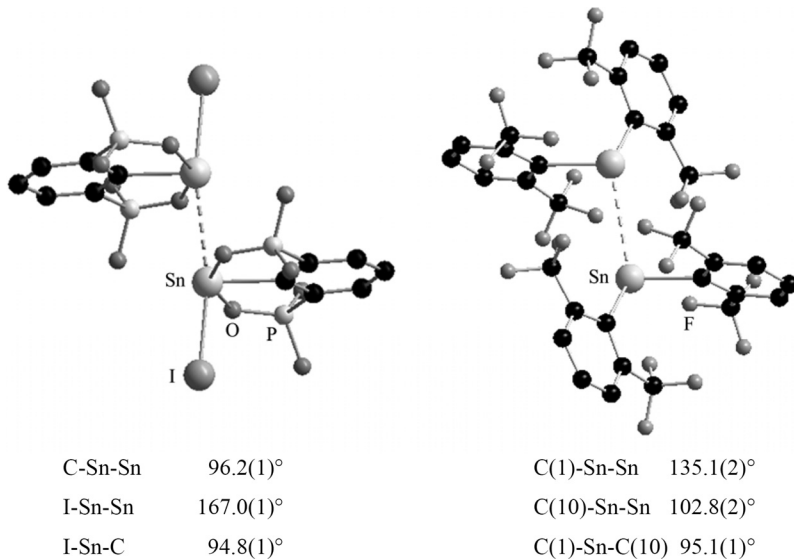


Figure 5. Schematic representation of the molecular structures of compound **5** (left) and of $[2,4,6-(\text{CF}_3)_3\text{C}_6\text{H}_2]_2\text{Sn}$ (right). For compound **5** the isopropyl and *tert*-butyl groups, and for $[2,4,6-(\text{CF}_3)_3\text{C}_6\text{H}_2]_2\text{Sn}$ the CF_3 group in 4-position are omitted for clarity.

The difference between the latter compound and the heteroleptic stannylenes **4** and **5** is (i) the formal replacement of one aryl substituent by a bromine respectively iodine atom and (ii) the presence of two strong intramolecular $P=O \rightarrow Sn$ interactions. The consequence of this is that there are dramatic differences in both the bond and torsion angles as it is illustrated in Figure 5.

The Mössbauer spectra of the organohalogenidostannylene **3** (I.S. $2.93 \text{ mm} \cdot \text{s}^{-1}$; Q.S. $3.30 \text{ mm} \cdot \text{s}^{-1}$), **4** (I.S. $3.02 \text{ mm} \cdot \text{s}^{-1}$; Q.S. $3.32 \text{ mm} \cdot \text{s}^{-1}$), and **5** (I.S. $3.07 \text{ mm} \cdot \text{s}^{-1}$; Q.S. $3.23 \text{ mm} \cdot \text{s}^{-1}$) confirm the divalent nature of the tin atoms in these compounds. Notably, the data for compound **3** differ considerably from those measured for the ethoxy-substituted analogue $[4-t\text{Bu}-2,6-\{P(O)(OEt)_2\}_2C_6H_2]SnCl$ (I.S. $3.24 \text{ mm} \cdot \text{s}^{-1}$, Q.S. $3.51 \text{ mm} \cdot \text{s}^{-1}$)^[10] and underline the structural difference between both compounds. The same statement holds for the ^{119}Sn MAS chemical shift of $\delta = -96$ (**3**) vs. $\delta = -160$ ($[4-t\text{Bu}-2,6-\{P(O)(OEt)_2\}_2C_6H_2]SnCl$).^[10] On the other hand, the Mössbauer data are not sensitive toward the structural differences between the organochloridostannylene **3** (monomeric) on the one hand and the organobromido- and organoiodidostannylene **4** and **5**, respectively, ($Sn \cdots Sn$ approach) on the other hand. Notably, the I.S.'s for $SnCl_2$ ($4.06 \text{ mm} \cdot \text{s}^{-1}$),^[15a] $SnBr_2$ ($3.95 \text{ mm} \cdot \text{s}^{-1}$),^[15b] and SnI_2 ($3.90 \text{ mm} \cdot \text{s}^{-1}$)^[15c] are larger and show the opposite trend with the biggest value found for $SnCl_2$. However, the I.S.-differences between **3** and **5** ($0.14 \text{ mm} \cdot \text{s}^{-1}$) and between $SnCl_2$ and SnI_2 ($0.16 \text{ mm} \cdot \text{s}^{-1}$) are rather similar.

The $Sn(1)$ atoms in the organostannylenes **3–5** and **6** exhibit ψ -trigonal bipyramidal configurations with $C(1)$, $X(1)$ (**3–5**, $X = Cl, Br, I$; **6**, $X = S$), and the lone pair occupying the equatorial, and $O(1)$, $O(2)$ occupying the axial positions. The stereochemical activity of the lone pair at $Sn(1)$ is especially manifested in the $C(1)-Sn(1)-X(1)$ bond angles ranging between $94.9(1)^\circ$ (**5**) and $89.4(1)^\circ$ (**6**). The former is close to that reported for $2,6-(Me_2NCH_2)_2C_6H_3SnCl$ ($95.0(3)^\circ$)^[1b] and the latter is the smallest value found among related derivatives containing a $CSnX$ fragment; the biggest value of $101.6(4)^\circ$ being reported for $[2-\{C(SiMe_3)_2\}C_5H_4N]SnCl$.^[1d] The $C(1)-Sn(1)-X(1)$ angles found for **3–5** and **6** hint at high s-character of the lone pair at $Sn(1)$ in these compounds. The $O(1)-Sn(1)-O(2)$ angles fall into the narrow range of $151.9(1)$ (**4**) and $152.5(1)^\circ$ (**6**). They are similar to the corresponding angle in $[4-t\text{Bu}-2,6-\{P(O)(OEt)_2\}_2C_6H_2]SnSiPh_3$ ($151.0(1)^\circ$)^[10] and are mainly the result of ligand constraint. The intramolecular $Sn(1)-O(1)/O(2)$ distances are rather similar and vary between $2.427(2)$ (**3**) and $2.478(2)$ Å (**6**). The two phosphorus atoms in **3–5** and **6** are crystallographically nonequivalent and, exemplarily, for compound **3** this is nicely reflected by a $^{31}\text{P}\{\text{H}\}$ MAS NMR (161.98 MHz) spectrum showing two equally intense resonances at $\delta = 33.2$ and 34.4 . The $C(1)-C(2)-P(1)/C(1)-C(6)-P(2)$ angles (α/α' angles)^[11h] between $114.9(2)$ (**6**) and $117.3(2)^\circ$ (**4**) support the idea that the $Sn-O$ interactions are attractive. Similar angles ($114.9(5)/114.5(3)^\circ$) were observed for the diorganotin dichloride $[4-t\text{Bu}-2,6-\{P(O)(OEt)_2\}_2C_6H_2]SnPhCl_2$.^[11o] As a result of the $O \rightarrow Sn$ coordination, the $P(1)-O(1)/P(2)-O(2)$ distances in **3–5** and **6** are longer than those of the protonated

ligand $5-t\text{Bu}-1,3-\{P(O)(OEt)_2\}_2C_6H_3$ (**2**, $1.469(3)/1.468(3)$ Å) and fall into the range between $1.483(2)$ (**3**) and $1.491(2)$ (**5**). Associated with this is the decrease of the $v(P=O)$ for **3** (1189 , 1162 cm^{-1}), and **6** (1193 , 1180 cm^{-1}) with respect to the protonated ligand **2** (1250 cm^{-1}). The $Sn(1)-Cl(1)$ distance in compound **3** amounts to $2.4708(8)$ Å and is comparable with the $Sn-Cl$ distances in $[2,6-(Me_2NCH_2)_2C_6H_3]SnCl$ ($2.488(3)$ Å),^[1b] $[2,6-Trip_2C_6H_3]SnCl \cdot Py$ ($2.448(2)$ Å),^[1p] and $[2-\{C(SiMe_3)_2\}C_5H_4N]SnCl$ ($2.440(5)$ Å).^[1d] The $Sn-Br$ distance of $2.6286(3)$ Å (**4**) is shorter than the corresponding distance in intramolecularly $N \rightarrow Sn$ coordinated $[Sn\{CH(SiMe_3)C_9H_6N-8\}Br]$ ($2.679(1)$ Å),^[8] whereas the $Sn-I$ distance of $2.8544(3)$ (**5**) Å is longer than the corresponding distance reported for $[Sn(I)\{C_6H_3-2,6-Trip_2\}]$ ($2.766(2)$ Å)^[11] with the tin atom of the latter being two-coordinate. The $Sn(1)-S(1)$ bond length in compound **6** of $2.512(1)$ Å resembles the corresponding $Sn-S$ distances of $2.532-2.552$ Å in the trithiophenolato stannates $[Ph_4E][Sn(SPh)_3]$ ($E = P,^[16] As^[17a])$

For both compounds **3** and **6**, the $Sn(1)$, $O(1)$, and $O(2)$ atoms are only slightly displaced from the plane defined by the aromatic carbon atoms (see torsion angles in Table 1).

The molecular structure of the organochloridoplumbylene **7** is shown in Figure 6. Selected bond lengths and bond angles are given in Table 1.

In contrast to the corresponding organochloridostannylene **3**, compound **7** shows almost the same μ -chlorido-bridged polymeric structure like its ethoxy-substituted analogue.^[11g] Minor differences between both structures are the slightly shorter $O(1)-Pb(1)$ distance of $2.518(2)$ Å and the more symmetric $Pb-Cl \cdots Pb$ bridge with $Pb(1)-Cl(1)$ and $Pb(1)-Cl(1A)$ distances of $2.836(1)$ and $2.879(1)$ Å, respectively, for compound **7**. A notable feature in the structure of compound **7** is the intramolecular $H(14) \cdots Cl(1)$ distance of $2.759(1)$ Å that is shorter than the sum of the van der Waals radii of chlorine ($1.70-1.90$ Å) and hydrogen ($1.20-1.45$ Å), which seems to influence the conformation of the $P-O-CH(CH_3)_3$ moiety.

The molecular structure of the organochloridostannylene chromiumpentacarbonyl complex **8** is shown in Figure 7. Se-

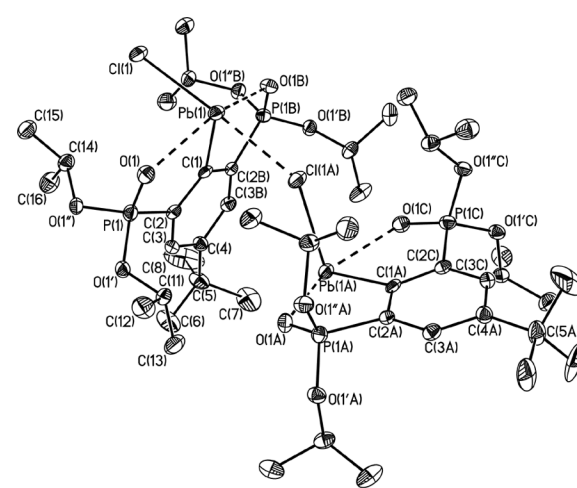


Figure 6. Molecular structure of compound **7**.

lected bond lengths and angles are given in the Figure caption.

The molecular structure of compound **8** strongly resembles that of its ethoxy-substituted analogue [4-*t*Bu-2,6-{P(O)(OEt)₂}₂C₆H₂]Sn(Cl)Cr(CO)₅.^[10] The tin atom shows a distorted trigonal bipyramidal configuration with the O(1) and

O(2) atoms occupying the axial, and the C(1), Cl(1) and Cr(1) atoms occupying the equatorial positions. Most remarkably, the intramolecular P=O→Sn interactions in compound **8** (O(1)–Sn(1) 2.316(2), O(2)–Sn(1) 2.347(2) Å) are stronger than in the parent stannylene **3** (O(1)–Sn(1) 2.430(2), O(2)–Sn(1) 2.427(2) Å) and indicate an enhanced Lewis acidity of the tin atom in the transition metal complex **8**.

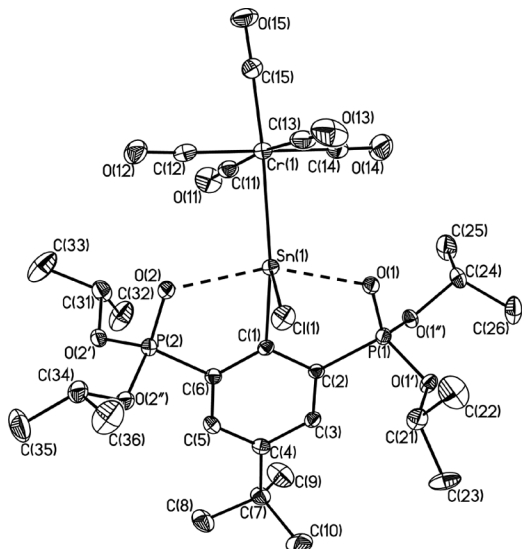
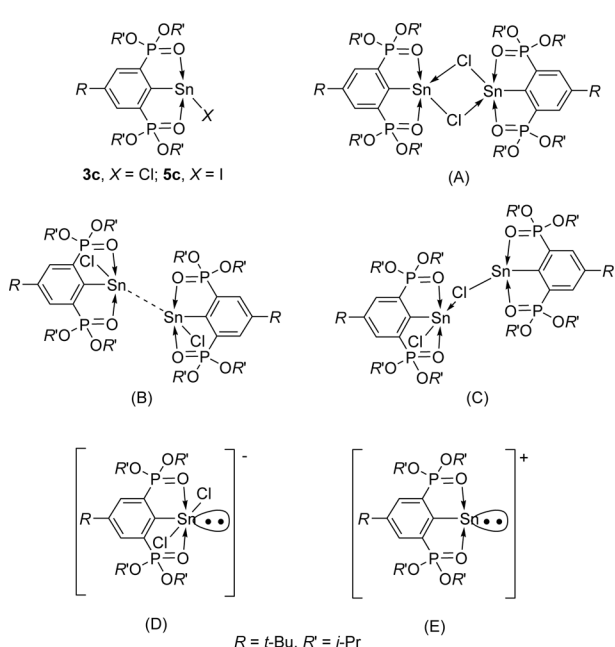


Figure 7. Molecular structure of compound **8**. Selected interatomic distances /Å: Sn(1)–C(1) 2.177(2), Sn(1)–Cl(1) 2.403(1), Sn(1)–Cr(1) 2.5783(4), Sn(1)–O(1) 2.316(2), Sn(1)–O(1) 2.347(2). Selected interatomic angles /deg: C(1)–Sn(1)–Cl(1) 97.54(6), C(1)–Sn(1)–Cr(1) 141.24(6), Cl(1)–Sn(1)–Cr(1) 121.14(2), O(1)–Sn(1)–O(2) 155.82(6), C(1)–C(2)–P(1) 115.2(2), C(1)–C(6)–P(2) 115.1(2). Selected torsion angles /deg: Sn(1)–C(1)–C(2)–C(3) 179.1(2), O(1)–P(1)–C(2)–C(3) –176.5(2), O(2)–P(2)–C(6)–C(5) –176.8(2).



Scheme 3. Schematic presentation of the different geometries for which MO calculations were performed. The lone electron pairs for **3c**, **5c**, and (A)–(C) are omitted for clarity.

DFT Calculations

The unusual tin–tin interaction in the solid state of two *RSnX* molecules (**4**, *X* = Br; **5**, *X* = I) raises the question for its energy and the factors that influence the latter. To probe alternative bonding modes we considered first the geometry optimization of the monomeric compounds *RSnX* (**3c**, *X* = Cl; **5c**, I, (Scheme 3).

Optimized geometric parameters of complexes **3c** and **5c** are listed in Table 2. The calculated distances *d*(Sn–*X*) of 2.524 Å (**3c**) and of 2.935 Å (**5c**), *d*(Sn)–C and *d*(Sn–O1), *d*(Sn–O2) and calculated angles of C–Sn–Cl of 90.7° and C–Sn–I of 92.9° are in good agreement with those obtained by X-ray diffraction analysis. The most predominant feature of the structure of both **3c** and **5c** is a bend of the halogenido ligand towards the aryl substituent due to the inert electron pair effect at the tin atom.

Table 2. Selected bond lengths /Å, bond angles, and torsion angles /deg for calculated monomeric (**3c** and **5c**) and dimeric structures **3cd** and **5cd**.

	3c (<i>X</i> = Cl)	5c (<i>X</i> = I)	3cd (<i>X</i> = Cl)	5cd (<i>X</i> = I)
Sn–Sn			3.758	3.704
Sn– <i>X</i>	2.509	2.902		2.935
<i>X</i> –Sn–Sn			1.718	1.661
Sn–C	2.295	2.293	2.280	2.277
<i>X</i> –Sn–C	90.2	92.4	90.7	92.9
Sn–O1	2.508	2.495	2.510	2.485
Sn–O2	2.488	2.490	2.480	2.491
O–Sn–O	151.2	151.2	152.0	152.0
H1–O1			2.670	2.535
H2–O2			2.650	2.672
P1–O1	1.510	1.510	1.513	1.513
P2–O2	1.510	1.510	1.511	1.513

For the calculation of the dimers two putative structures were taken into account. A dichlorido-bridged four-membered ring **A** (Scheme 3) and a geometry **B** (Scheme 3) with a tin–tin bridge actually found in the solid state for compounds **4** and **5**. The geometry optimization of the **A** type dimer with chlorido bridges resulted in Sn–Cl···Sn bond dissociation and formation of two monomeric complexes **3c**.

We therefore considered the **B** type dimers **3cd** and **5cd** as the most likely structure for the dimerization of two *RSnX* (*X* = Cl, I) moieties. Geometry optimization revealed the geometry parameters listed in Table 2 with calculated energies that are 16 and 20 kJ·mol⁻¹ below the energy of two monomeric *RSnCl* and *RSnI* species, respectively. Thus, the formation of dimers **3cd** and **5cd** is energetically favorable but apparently the binding energy is very low and, especially for the chlorido-substi-

tuted compound **3**, might be compensated for by interactions with solvent molecules in solution and by packing forces in the solid state.

To gain further insights into the unusual Sn···Sn bonding we analyzed the orbital contributions from each *RSnX* fragment. A molecular orbital analysis revealed an interaction diagram for two monomeric compounds **3c** to a dimer **3cd** (Supporting Information, Figure S3). The main interaction results from two filled fragment orbitals which can be assigned as lone pairs of the Sn^{II} fragment. The interaction of the two occupied orbitals results in a 2-center-4-electron repulsion which is stabilized by a mixing from the empty antibonding Sn–*X* orbitals. The degree of mixing depends on the electronegativity of the substituent *X*. It is slightly larger for *X* = I than for *X* = Cl. Thus, the Sn–Sn bonding interaction becomes stronger for *X* = I. In addition, a short C–H···O interaction of 2.395(2) Å between the methine proton of one of the isopropoxy substituents and the Sn–O–P bridging oxygen atom was found in the solid-state structure of complex **5** as determined by single crystal X-ray diffraction analysis as well as in the optimized structure of complex **5cd** (2.507 Å). This interaction might contribute to the stability of the dimer in complex **3cd** as well as **5cd**.

Interestingly, the availability of the antibonding Sn–*X* orbitals also depends on the presence of intramolecular P=O→Sn interaction. Thus, the DFT calculation-based geometry optimization for the hypothetical model compound *p*-*t*BuC₆H₄SnI in which the two phosphonyl moieties, P(O)(O-*i*Pr)₂, had been removed revealed an iodido-bridged dimer (Figure S2, Supporting Information) rather than a Sn···Sn interaction.

Structures in Solution

In solution, the arydiphosphonic ester **2** as well as the organostannylanes **3–5** and **6** are essentially monomeric. The ¹H NMR spectrum (C₆D₆, 599.83 MHz) of compound **2** showed a singlet resonance for the *tert*-butyl protons, a multiplet for the methine protons, *AA'*XX' and *AB₂X₂* resonances for the aromatic protons and most importantly, two doublet resonances of equal integral at δ = 1.02 ($^3J(^1\text{H}-^1\text{H})$ 6.3 Hz) (a) and δ = 1.17 ($^3J(^1\text{H}-^1\text{H})$ 6.3 Hz) (b) that are assigned to nonequivalent methyl protons of the isopropoxy groups. NOE experiments reveal the low-frequency shifted doublet (a) to belong to those methyl protons being close to the aromatic protons.

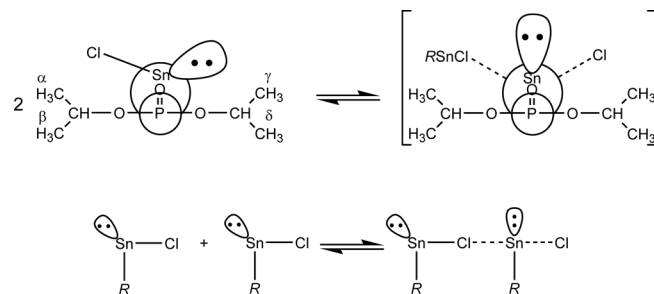
The ¹H NMR spectrum (C₆D₆ or [D₈]toluene, 599.83 MHz) of the organochloridostannylene **3** is both concentration- and temperature-dependent. Thus, at room temperature the spectrum of a medium-concentrated sample (12 mg/0.6 mL [D₈]toluene) is similar to that of compound **2**, except that there is no *AB₂X₂*-type resonance and that the doublet at δ = 1.25 is slightly broadened in comparison to that at δ = 0.97. At -17 °C the signal at δ = 1.25 de-coalesced into two equally intense doublets at δ = 1.34 ($^3J(^1\text{H}-^1\text{H})$ 6.1 Hz) and 1.16 ($^3J(^1\text{H}-^1\text{H})$ 6.1 Hz), respectively, whereas the doublet at δ = 0.97 ($^3J(^1\text{H}-^1\text{H})$ 6.0 Hz) remained virtually unchanged. Simultaneously, the signal for the methine protons de-coalesced into two broad and equally intense resonances at δ = 4.90 and 5.36, respectively. Most importantly, the same de-coalescence phenomena were

observed at room temperature upon dilution of the sample. The ¹H NMR spectrum of a diluted sample (1 mg/0.6 mL [D₈]toluene) measured at 599.83 MHz even showed complete de-coalescence into four equally intense doublets for the methyl protons of the isopropoxy groups. Addition of tetraphenylphosphonium chloride, Ph₄PCl, to this solution again caused coalescence of the four doublets into two doublets.

The ¹¹⁹Sn NMR spectrum (149.21 MHz, [D₈]toluene) of compound **3** showed a triplet resonance at δ = -99 ($J(^{119}\text{Sn}-^{31}\text{P})$ 121 Hz) which, upon cooling of the solution to -85 °C, broadened and shifted to δ = -114 ($\nu_{1/2}$ 500 Hz). Addition of one molar equivalent of Et₄NCl caused no change of the chemical shift, neither at room temperature nor at -85 °C. The ³¹P NMR spectrum (161.98 MHz) is virtually temperature- and solvent-independent and displayed resonances at δ = 37.5 ($J(^{31}\text{P}-^{119}\text{Sn})$ 120 Hz, [D₈]toluene, T = 25 °C), δ = 38.3 ($J(^{31}\text{P}-^{119}\text{Sn})$ 114 Hz, [D₈]toluene, T = -85 °C), and δ = 38.1 ($J(^{31}\text{P}-^{119}\text{Sn})$ 117 Hz, [D₈]THF, T = -85 °C), respectively.

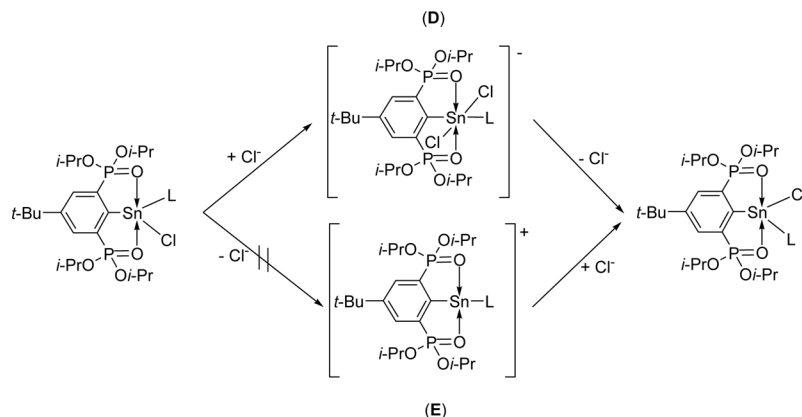
In contrast to the organochloridostannylene **3**, the ¹H NMR spectrum ([D₈]toluene, 599.83 MHz) of the thiophenolato-substituted derivative **6** does not show coalescence phenomena upon variation of temperature and/or concentration. Thus, at ambient temperature four doublets at δ = 0.95 ($^3J(^1\text{H}-^1\text{H})$ 6.0 Hz), 1.05 ($^3J(^1\text{H}-^1\text{H})$ 6.0 Hz), 1.16 ($^3J(^1\text{H}-^1\text{H})$ 6.0 Hz), and 1.33 ($^3J(^1\text{H}-^1\text{H})$ 6.0 Hz) were observed for the methyl protons of the isopropoxy groups, and two multiplet signals centered at δ = 4.46 and 5.23, respectively, for the methine (CH) protons. The ³¹P and ¹¹⁹Sn NMR spectra each displayed a single resonance at δ = 35.3 ($J(^{31}\text{P}-^{119}\text{Sn})$ 98 Hz) and δ = -2 ($J(^{119}\text{Sn}-^{31}\text{P})$ 98 Hz), respectively.

These results indicate the dynamic process to account for the coalescence phenomena in the ¹H NMR spectra of compound **3** to take place at the tin rather than at the phosphorus atom and to involve the equilibria shown in Scheme 4 (for absence of additional chloride ions) and Scheme 5 (presence of additional chloride ions).



Scheme 4. Schematic view along the P···Sn axis (above) and the equilibrium that accounts for the concentration dependence of the coalescence phenomena (below).

For the organothiophenolatostannylene **6** the equilibrium (Scheme 4) is slow (or even absent) on the ¹H NMR time scale and consequently, the α-, β-, γ-, and δ-methyl protons are non-equivalent (Scheme 4). For the organochloridostannylene **3**, the equilibrium (Scheme 4) is fast at ambient temperature and/or at high concentration. The α- and γ-, and the β- and δ-methyl protons become equivalent resulting in observation of



Scheme 5. Proposed mechanism that accounts for the configurational instability of compounds **3** ($L = \text{lone pair}$) and **8** [$L = \text{Cr}(\text{CO})_5$] in presence of chloride anion.

two equally intense doublets. At low concentration and/or low temperature the equilibrium becomes slow on the ^1H NMR time scale giving rise to de-coalescence of the α - and γ -methyl proton resonances into two equally intense doublets. DFT calculations reveal that the monochlorido-bridged dimer **C** (Scheme 3) lies in a thermodynamic minimum (in contrast to the dichlorido-bridged dimer **A** in Scheme 3) being only $5.4 \text{ kJ}\cdot\text{mol}^{-1}$ higher in energy than two separate monomers.

In the presence of additional chloride anions, the equilibrium according to Scheme 5 is fast even at rather low concentration. Important to notice is that the concentration of both the dimer (equilibrium shown in Scheme 4) and the organodichloridostannite (**D**) (equilibrium shown in Scheme 5) is rather low and contributes only negligibly to the ^{119}Sn NMR chemical shift actually observed. Formation of an organotin(II) cation (**E**) by loss of chloride ion (Scheme 3, Scheme 5) would also cause coalescence. However, DFT calculations show that this process requires much more energy ($517 \text{ kJ}\cdot\text{mol}^{-1}$) than formation of the organodichloridostannite **D** ($133 \text{ kJ}\cdot\text{mol}^{-1}$, Scheme 3, Scheme 5). With respect to these calculations it is worth mentioning that the electrospray mass spectrum (positive mode) of the organochloridostannylene **3** showed a mass cluster centered at $m/z = 581$ that corresponds to $[4-t\text{Bu}-2,6-\{\text{P}(\text{O})(\text{O}i\text{Pr})_2\}_2\text{C}_6\text{H}_2]\text{Sn}^+$ whereas in the negative mode no mass cluster corresponding to the organodichloridostannite anion $[4-t\text{Bu}-2,6-\{\text{P}(\text{O})(\text{O}i\text{Pr})_2\}_2\text{C}_6\text{H}_2]\text{SnCl}_2^-$ was detected. Apparently, under ESI-MS conditions cations show up more easily than anions do.

The equilibrium shown in Scheme 4 gets support from (i) the ^{31}P NMR spectrum of an equimolar mixture of the organochloridostannylene **3** ($\delta = 37.8$) and the organoiodidostannylene **5** ($\delta = 36.9$) to show one broad resonance at $\delta = 37.2$ indicating fast exchange, and (ii) the ^{31}P NMR spectrum of an equimolar mixture of **3** and the organothiophenolatostannylene **6** to show two resonances at $\delta = 37.8$ and $\delta = 35.4$, respectively, indicating slow (or no) exchange. Furthermore, the chromiumpentacarbonyl-substituted organostannylene **8** is configurationally stable and shows in its ^1H NMR spectrum regardless of the concentration four equally intense doublet resonances for the methyl protons of the isopropoxy substitu-

ents. Apparently, for this compound, like for the organothiophenolatostannylene **6**, any association is precluded by steric hindrance. However, coalescence of these four doublet resonances into one doublet at $\delta = 1.18$ ($J^{1\text{H}-1\text{H}}$ 6.0 Hz) and a rather broad ($v_{1/2}$ 67 Hz) signal at $\delta = 0.95$ (just coalescing), and a broadening (pre-coalescence) of the two methine resonances was achieved by addition of tetraphenylphosphonium chloride, Ph_4PCl . It clearly indicates the mechanism shown in Scheme 5 to be operative.

Finally, direct evidence for the absence of a dissociative mechanism for the configurational lability of the tin atom in intramolecularly coordinated organostannlenes of the type $[4-t\text{Bu}-2,6-\{\text{P}(\text{O})(\text{O}i\text{Pr})_2\}_2\text{C}_6\text{H}_2]\text{Sn}X$ ($X = \text{electronegative substituent such as halogen, alkoxide, thiolate, amide}$) stems from the ^{19}F and ^{119}Sn NMR spectra of the organofluoridostannylene $[4-t\text{Bu}-2,6-\{\text{P}(\text{O})(\text{O}i\text{Pr})_2\}_2\text{C}_6\text{H}_2]\text{SnF}$ that was prepared *in situ* by the reaction of the organotin(II) amide $[4-t\text{Bu}-2,6-\{\text{P}(\text{O})(\text{O}i\text{Pr})_2\}_2\text{C}_6\text{H}_2]\text{SnN}(i\text{Pr})_2$ with ammonium fluoride, NH_4F . The ^{19}F and ^{119}Sn NMR spectra displayed a singlet resonance at $\delta = -138.4$ ($J^{19\text{F}-117/119\text{Sn}}$ 3051/3194 Hz) and a doublet of triplet resonance at $\delta = -202$ ($J^{119\text{Sn}-^{19}\text{F}}$ 3191, $J^{119\text{Sn}-^{31}\text{P}}$ 108 Hz), respectively. The $J^{119\text{Sn}-^{19}\text{F}}$ coupling constant is close to that recently reported for LSnF [$L = \text{HC}(\text{CMeNAr})_2$, Ar = $2,6-i\text{Pr}_2\text{C}_6\text{H}_3$].^[1s] Details for the synthesis of $[4-t\text{Bu}-2,6-\{\text{P}(\text{O})(\text{O}i\text{Pr})_2\}_2\text{C}_6\text{H}_2]\text{SnF}$ will be presented in a forthcoming paper.

Conclusions

In this work we report the syntheses and structures in solution and in the solid state of a series of intramolecularly coordinated heteroleptic organostannlenes of the type $[4-t\text{Bu}-2,6-\{\text{P}(\text{O})(\text{O}i\text{Pr})_2\}_2\text{C}_6\text{H}_2]\text{Sn}(X)L$ ($X = \text{Cl}, \text{Br}, \text{I}, \text{SPh}; L = \text{lone pair}, \text{Cr}(\text{CO})_5$) and of the organoplumbylene $[4-t\text{Bu}-2,6-\{\text{P}(\text{O})(\text{O}i\text{Pr})_2\}_2\text{C}_6\text{H}_2]\text{PbCl}$. We learned that the tin atom in the organochloridostannylene **3** ($X = \text{Cl}, L = \text{lone pair}$) is configurationally not stable whereas the thiophenolato-substituted derivative **6** ($X = \text{SPh}, L = \text{lone pair}$) and the chromiumpentacarbonyl complex **8**, under the same conditions, do not show exchange of configuration at the tin atom. NMR spectroscopy

at variable temperature and concentration as well as DFT calculations make an associative mechanism to account for the configurational lability of compound **3** very likely, rather than a dissociative one. This supports the interpretation made by *van Koten* et al. for the dynamic behavior of the organostannylene ($2,6\text{-Me}_2\text{NCH}_2)_2\text{C}_6\text{H}_3\text{SnCl}$,^[1b,10] the findings by *Lappert* et al. on the halide exchange in β -diketiminato(tin(II)) halides^[17b] and our previous results on the ethoxy-substituted heteroleptic organostannylene [$4\text{-}t\text{Bu-2,6-}\{\text{P(O)(OEt)}_2\}_2\text{C}_6\text{H}_2\text{SnCl}$.^[10]

Most importantly, the association behavior in the solid state of [$4\text{-}t\text{Bu-2,6-}\{\text{P(O)(OR)}_2\}_2\text{C}_6\text{H}_2\text{SnX}$] ($R = \text{Et, } i\text{Pr; } X = \text{Cl, Br, I, SPh}$) depends on the identity of both R and X . Whereas the ethoxy-substituted organochloridostannylene ($R = \text{Et, } X = \text{Cl}$) is more likely a chlorido-bridged dimer or polymer, its isopropoxy-substituted analogue **3** ($R = i\text{Pr, } X = \text{Cl}$) is a monomer. On the other hand, the bromido ($R = i\text{Pr, } X = \text{Br}$) and iodido ($R = i\text{Pr, } X = \text{I}$) substituted derivatives **4** and **5** are dimers with weak tin–tin interactions. As suggested by MO calculations, the latter are made possible by participation of empty Sn– X ($X = \text{Cl, I}$) σ^* orbitals the availability of which is higher for $X = \text{I}$ than $X = \text{Cl}$, and which is influenced by the presence of intramolecular donor–acceptor interactions such as $\text{P=O}\rightarrow\text{Sn}$ in compounds **3–6**, and $\text{CF}_3\rightarrow\text{Sn}$ in [$2,4,6\text{-}(\text{CF}_3)_3\text{C}_6\text{H}_2\text{Sn}$].^[14] The weak secondary bond thus formed between two Sn^{II} atoms is supported by nonbonding interactions as well as weak van der Waals interactions.

Notably, it appears that the concept can be generalized for weak interactions between organo compounds of low-valent heavy elements. Thus, recently *Beckmann* et al. reported the solid-state structures of the organotellurium compounds $2,4,6\text{-}t\text{Bu}_3\text{C}_6\text{H}_2\text{TeCl}$ ^[17c] and $8\text{-Me}_2\text{NC}_{10}\text{H}_6\text{TeCl}$ ^[17d] that have a rather similar substituent pattern but differ by the absence respectively presence of an intramolecular $\text{N}\rightarrow\text{Te}$ interaction. The former compound is a chlorido-bridged polymer whereas the latter compound shows a weak Te···Te interaction at a distance of $3.87(1)$ Å.

Experimental Section

General: All solvents were dried and purified by standard procedures. All reactions were carried out in an atmosphere of dry argon. Varian INOVA 600, Bruker DRX400, Bruker DRX500 and Bruker DPX-300 spectrometers were used to obtain ^1H , ^{13}C , ^{31}P , and ^{119}Sn NMR spectra. ^1H , ^{13}C , ^{31}P , and ^{119}Sn NMR chemical shifts are given in ppm and were referenced to Me_4Si , H_3PO_4 (85 %, ^{31}P) and Me_4Sn (^{119}Sn). The ^{31}P CP-MAS and ^{119}Sn CP-MAS spectra were recorded with a Bruker Avance 400 spectrometer at room temperature. CP/MAS (cross-polarization/magic angle spinning) experiments were used with repetition delays of 8 s (^{31}P) and 10 s (^{119}Sn), and the contact times were set at 7 ms (^{31}P) and 10 ms (^{119}Sn). Three spinning rates (3000, 5000, 8000 Hz, ^{31}P ; 6000, 7000, 9000 Hz, ^{119}Sn) were used to identify the isotropic chemical shift. The ^{31}P and ^{119}Sn chemical shifts were calibrated using H_3PO_4 (85 %) and tetracyclohexyltin ($\delta = -97.35$), respectively. The IR spectra were recorded with a Bruker IFS 28 spectrometer. The Mössbauer spectra were recorded in constant-acceleration mode with a home-made instrument, designed and built by the Instituut voor Kern- en Stralingsfysica (IKS), Leuven. The isomer shifts refer to a source of $\text{Ca}^{119m}\text{SnO}_3$ from Amersham, UK, sam-

ples being maintained at 90 ± 2 K. The data were treated with a least-square iterative program deconvoluting the spectrum into a sum of lorentzians.

The electrospray mass spectra were recorded on a Thermoquest-Finnigan instrument using CH_3CN as the mobile phase. The samples were introduced as solution in CH_3CN via a syringe pump operating at a rate of $0.5 \mu\text{L}\cdot\text{min}^{-1}$. The capillary voltage was 4.5 kV while the cone skimmer voltage varied between 50 and 250 kV. Identification of the expected ions was assisted by comparison of experimental and calculated isotope distribution patterns. The m/z values reported correspond to those of the most intense peak in the corresponding isotope pattern. Elemental analyses were performed with a LECO-CHNS-932 analyzer.

X-ray Crystallography

Intensity data for the colorless crystals were collected with a Nonius KappaCCD diffractometer with graphite-monochromated $\text{Mo}-K_{\alpha}$ (0.71073 Å) radiation at $173(1)$ K. The data collection covered almost the whole sphere of reciprocal space with two (**3**), three (**2**, **4**, **6**, **7**), four (**8**), and five (**5**) sets at different κ -angles with 317 (**2**), 194 (**3**), 288 (**4**), 395 (**5**), 234 (**6**), 230 (**7**), and 418 (**8**) frames via ω -rotation ($\Delta/\omega = 1^\circ$) at two times 10 s (**8**), 20 s (**4**, **5**), 30 s (**3**), 90 s (**2**), 125 s (**7**), and 150 s (**6**) per frame. The crystal-to-detector distance was 3.4 cm (**2**, **4–8**) and 4.0 cm (**3**). Crystal decay was monitored by repeating the initial frames at the end of data collection. The data were not corrected for absorption effects. Analyzing the duplicate reflections there was no indication for any decay. The structure was solved by direct methods SHELXS97^[18] and successive difference Fourier syntheses. Refinement applied full-matrix least-squares methods SHELXL97.^[19]

Only the positions of H(1), H(3), and H(5) in compound **2** were refined whereas all other hydrogen atoms were placed in geometrically calculated positions using a riding model with isotropic temperature factors constrained at 1.2 for non-methyl and at 1.5 for methyl groups times U_{eq} of the carrier carbon atom.

In **3** isopropoxy and *tert*-butyl groups are disordered over two sites with occupancies of 0.4 (C(8'), C(9'), C(10'), C(15'), C(16')) of 0.5 (C(12), C(13), C(12'), C(13'), C(25), C(26), C(25'), C(26')) and 0.6 (C(8), C(9) C(10), C(15), C(16)) and in **8** an isopropoxy group with occupancies of 0.4 (C(23') and 0.6 (C(23)). The solvent molecule toluene in **8** was refined with an occupancy of 0.5 and a set of restraints to aid in modeling the disorder (AFIX 66 for aromatic rings and DFIX 1.540(1) for methyl aryl distances).

Atomic scattering factors for neutral atoms and real and imaginary dispersion terms were taken from International Tables for X-ray Crystallography.^[20] The figures were created by SHELXTL.^[21] Crystallographic data are given in Table 3.

Crystallographic data for the structure reported in this paper have been deposited with the Cambridge Crystallographic Data Centre as supplementary material publications no. CCDC-801082 (2), -801081 (3), -801085 (4), -801086 (5), -801084 (6), -801087 (7), -801083 (8). Copies of the data can be obtained free of charge on application to CCDC, 12 Union Road, Cambridge, CB2 1EZ, UK (Fax: +44-1223-336033; E-Mail: deposit@ccdc.cam.ac.uk).

Computational Details

For all calculations on the density functional theory level, the Program Turbomole was used.^[22] Energies and geometries were developed on

Table 3. Crystallographic data for compounds 2–8.

	2	3	4	5	6	7	8
formula	C ₂₂ H ₄₀ O ₆ P ₂	C ₂₂ H ₃₉ ClO ₆ P ₂ Sn	C ₂₂ H ₃₉ BrO ₆ P ₂ Sn	C ₂₂ H ₃₉ IO ₆ P ₂ Sn	C ₂₈ H ₄₄ O ₆ P ₂ SSn	C ₂₂ H ₃₉ ClO ₆ P ₂ Pb	C ₂₇ H ₃₉ ClCrO ₁₁ P ₂ Sn·0.5C ₇ H ₈
fw	462.48	615.61	660.07	707.06	689.32	704.11	853.73
cryst syst	triclinic	orthorhombic	monoclinic	monoclinic	monoclinic	orthorhombic	triclinic
cryst size /mm	0.08 × 0.08 × 0.05	0.13 × 0.10 × 0.10	0.24 × 0.20 × 0.20	0.22 × 0.22 × 0.20	0.05 × 0.05 × 0.05	0.10 × 0.10 × 0.06	0.20 × 0.20 × 0.18
space group	<i>P</i> ī	<i>P</i> 2 ₁ 2 ₁ 2 ₁	<i>P</i> 2 ₁ /c	<i>P</i> 2 ₁ /c	<i>P</i> 2 ₁ /c	<i>P</i> ma	<i>P</i> ī
<i>a</i> /Å	9.5782(4)	10.6527(2)	13.2715(5)	13.4089(6)	19.7239(9)	10.2171(4)	10.8903(2)
<i>b</i> /Å	11.3408(4)	16.4053(3)	12.5282(7)	12.5379(6)	9.8231(4)	18.886(1)	11.2655(2)
<i>c</i> /Å	13.2396(7)	17.0227(3)	18.3363(7)	18.4434(7)	18.1094(8)	15.1732(9)	16.3422(3)
<i>α</i> /deg	79.8412(2)	90	90	90	90	90	86.1897(7)
<i>β</i> /deg	89.1412(2)	90	105.180(3)	105.136(2)	107.344(2)	90	84.5212(8)
<i>γ</i> /deg	66.130(2)	90	90	90	90	90	78.5213(7)
<i>V</i> /Å ³	1292.0(1)	2974.90(9)	2942.4(2)	2993.1(2)	3349.2(3)	2927.8(3)	1953.55(6)
<i>Z</i>	2	4	4	4	4	4	2
ρ _{calcd.} /Mg·m ⁻³	1.189	1.374	1.490	1.569	1.367	1.597	1.451
μ /mm ⁻¹	0.200	1.086	2.366	2.022	0.956	5.994	1.118
<i>F</i> (000)	500	1264	1336	1408	354	1392	870
θ range /deg	2.96 to 27.55	3.13 to 27.48	2.92 to 27.47	2.91 to 27.48	2.98 to 25.35	2.63 to 27.48	2.02 to 27.48
index ranges	-12 ≤ <i>h</i> ≤ 12	-13 ≤ <i>h</i> ≤ 13	-17 ≤ <i>h</i> ≤ 17	-17 ≤ <i>h</i> ≤ 17	-23 ≤ <i>h</i> ≤ 22	-13 ≤ <i>h</i> ≤ 13	-14 ≤ <i>h</i> ≤ 14
	-12 ≤ <i>k</i> ≤ 14	-21 ≤ <i>k</i> ≤ 21	-16 ≤ <i>k</i> ≤ 16	-16 ≤ <i>k</i> ≤ 16	-11 ≤ <i>k</i> ≤ 11	-24 ≤ <i>k</i> ≤ 24	-13 ≤ <i>k</i> ≤ 14
	-17 ≤ <i>l</i> ≤ 17	-22 ≤ <i>l</i> ≤ 22	-23 ≤ <i>l</i> ≤ 22	-23 ≤ <i>l</i> ≤ 23	-21 ≤ <i>l</i> ≤ 21	-19 ≤ <i>l</i> ≤ 19	-20 ≤ <i>l</i> ≤ 21
no. of reflns colld	12924	18250	26849	37446	23080	21374	25780
completeness to θ _{max}	98.0	99.2	99.8	99.8	99.6	99.9	99.4
no. of indep reflns/ <i>R</i> _{int}	5843 / 0.077	6617 / 0.031	6734 / 0.033	6844 / 0.036	6100 / 0.065	3454 / 0.041	8901 / 0.034
no. of reflns obsd	2849	3780	4007	4161	3314	1855	6060
with [<i>I</i> > 2σ(<i>I</i>)]							
no. of refined Params	291	370	300	300	354	173	448
GooF (<i>F</i> ²)	0.992	0.709	0.773	0.834	0.801	0.657	0.913
<i>R</i> 1 (<i>F</i>) [<i>I</i> > 2σ(<i>I</i>)]	0.0771	0.0249	0.0279	0.0273	0.0352	0.0248	0.0354
<i>wR</i> 2 (<i>F</i>) (all data)	0.2229	0.0400	0.0422	0.0427	0.0556	0.0380	0.0582
(Δσ) _{max}	0.001	0.001	<0.001	0.001	0.001	0.001	0.001
largest diff. peak/hole / e·Å ⁻³	0.875 / -0.401	0.337 / -0.364	0.504 / -0.821	0.575 / -1.287	0.561 / -0.453	1.058 / -1.775	0.532 / -0.477

the nonlocal level of theory. For geometry optimization the energies were corrected for nonlocal exchange according to Becke^[23,24] and for nonlocal correlation according to Perdew (BP-86)^[25] in the self-consistent procedure. The TZVPPP-split valence base set was used for chlorine, bromine, phosphorus, oxygen, carbon and hydrogen atoms.^[26,27] For tin and iodine we used an effective core potential base set (ECP-28-mwb) with triple-zeta functions for the valence region and an additional d polarization function supplied by the program. For the *J*_{ij} term approximation an additional auxiliary base set was used.^[22,28] All stationary points were checked by second derivative calculations revealing no imaginary frequency for the minima.

For inclusion of dispersion (van der Waals) effects in the investigation of the Sn···Sn dimers single-point calculations using the functional B97-d^[29] were employed on previously optimized geometries. For the calculation of the species C, D and E, a TZVPP-split valence basis set was used.^[30]

Syntheses

1-Bromo-3-diisopropoxyphosphonyl-5-tert-butylbenzene (1): 1,3-Dibromo-5-tert-butylbenzene (39.6 g, 140 mmol) and nickel bromide, NiBr₂, (1.7 g, 7.8 mmol) were heated at 165 °C. Triisopropyl phosphite, P(O-iPr)₃, (35 mL, 140 mmol) was added dropwise within 30 min and the reaction mixture was kept at 165 °C for another 180 min, during which it turned black. The crude product was purified by column chromatography (silica, diethyl ether) to give 16.4 g (32 %) of compound 1 as brown oil. ¹H NMR (300.13 MHz, CDCl₃): δ = 1.20 (d, ³J¹H–¹H) = 6.2 Hz, 6 H), 1.29 (s, 9 H, C(CH₃)), 1.34 (d, ³J¹H–¹H) = 6.2 Hz, 6 H), 4.66 (doublet of septets, ³J¹H–¹H) = 6, ³J¹H–³¹P) = 9 Hz, 2 H, CH(CH₃)₂), 7.62–7.73 (complex pattern, aromatic H, 4 H). ³¹P{¹H} NMR (121.49 MHz, CDCl₃): δ = 16.1. No elemental analysis was performed.

5-*t*Bu-1,3-bis(diisopropoxyphosphonyl)benzene, 5-*t*Bu-1,3-[P(O)(O-iPr)₂]₂C₆H₃ (2): Within 2.5 h and at 160 °C, triisopropyl phosphite

(60 mL, 240 mmol) was added to a magnetically stirred suspension of 1,3-dibromo-5-tert-butylbenzene (30.0 g, 102 mmol) and NiBr₂ (4.5 g, 21 mmol). The dark brown suspension thus obtained was kept at 160 °C for additional 2 hrs during which the isopropyl bromide formed (17.8 g, 145 mmol) was condensed into a dry ice-cooled trap. After the crude reaction product had been pre-purified by column chromatography (silica gel/chloroform) it was distilled in vacuo to give 31.0 g (67 %) 5-*t*Bu-1,3-[P(O)(O-iPr)₂]₂C₆H₃ as colorless viscous oil that immediately solidified (m.p. 64–65 °C). ¹H NMR (400.13 MHz, C₆D₆): δ = 1.02 (d, 12 H, CH(CH₃)(CH₃)), ³J¹H–¹H) = 6.3 Hz), 1.06 (s, 9 H, C(CH₃)₃), 1.17 (d, 12 H, CH(CH₃)(CH₃)), ³J¹H–¹H) = 6.3 Hz), 4.68 (unresolved multiplet, 4 H, CH(CH₃)₂), 8.32 (AA'XX', 2 H, H4, H6), 8.59 (t, 1 H, ³J³¹P–¹H) = 20.5 Hz, H2). ¹³C{¹H} NMR (100.63 MHz, CDCl₃): δ = 23.8 (s, CH(CH₃)(CH₃)), 24.1 (s, CH(CH₃)(CH₃)), 31.2 (s, C(CH₃)₃), 35.1 (s, C(CH₃)₃), 70.9 (s, CH(CH₃)₂), 130.2 (dd, C1, C3, ¹J¹³C–³¹P) = 188.6, ³J¹³C–³¹P) = 14.6 Hz), 132.1–132.6 (complex pattern, C2, C4/6), 151.6 (t, C5, ²J¹³C–³¹P) = 26.2 Hz). ³¹P{¹H} NMR (161.98 MHz, CDCl₃): δ = 17.3. IR (KBr): ν(P=O) = 1250 cm⁻¹. Elemental analysis: C₂₂H₄₀P₂O₆ (462.23 g·mol⁻¹); C 57.2 (caled. 57.13); H 8.5 (8.72)%.

{[2,6-Bis(diisopropoxyphosphonyl)-4-tert-butylphenyl]tin(II) chloride, {4-*t*Bu-2,6-[P(O)(O-iPr)₂]₂C₆H₂}SnCl (3): A 0.75 M solution (36 mL, *n*-hexane/diethyl ether: 1/0.8) of lithium diisopropyl amide (27.5 mmol) was added dropwise within 20 min and at -60 °C to a solution of 4-*t*Bu-2,6-[P(O)(O-iPr)₂]₂C₆H₃ (10.3 g, 22.2 mmol) in THF (80 mL). After stirring the reaction mixture for 7 h at -40 °C, within 30 min, SnCl₂ (4.7 g, 24.8 mmol) was added in small portions. The reaction mixture was allowed to warm to room temperature overnight. After evaporating the solvents in vacuo the residue was extracted with hot *n*-hexane (3 × 100 mL) to provide 11.1 g (81 % yield) of compound 3 as colorless crystals of mp. 132 °C, suitable for X-ray diffraction analysis. ¹H NMR (300.13 MHz, C₆D₆): δ = 1.04 (d, 12 H, CH(CH₃)₂, ³J¹H–¹H) = 6.2 Hz), 1.17 (s, 9 H, C(CH₃)₃), 1.30 (d, 12 H, CH(CH₃)₂, ³J¹H–¹H) = 5.9 Hz), 4.90 (m, 4 H, CH(CH₃)₂, ³J¹H–¹H) = 6.1, ³J¹H–³¹P) = 7.3 Hz), 8.08 (d, 2 H, H3/5, ³J³¹P–¹H) =

13.0 Hz). $^{13}\text{C}\{\text{H}\}$ NMR (75.47 MHz, C_6D_6): $\delta = 23.4$ (d, $\text{CH}(\text{CH}_3)(\text{CH}_3)'$, $J^{(13)\text{C}-31\text{P}} = 5.4$ Hz), 23.8 (d, $\text{CH}(\text{CH}_3)(\text{CH}_3)'$, $J^{(13)\text{C}-31\text{P}} = 3.6$ Hz), 30.7 (s, $\text{C}(\text{CH}_3)_3$), 34.5 (s, $\text{C}(\text{CH}_3)_3$), 72.1 (s, $\text{CH}(\text{CH}_3)_2$), 131.6 (dd, C_3/C_5 , $^2J^{(13)\text{C}-31\text{P}} = 16.7$, $^4J^{(13)\text{C}-31\text{P}} = 4.4$ Hz), 132.6 (dd, C_2/C_6 , $^1J^{(13)\text{C}-31\text{P}} = 192.2$, $^3J^{(13)\text{C}-31\text{P}} = 23.6$ Hz), 150.9 (t, C_4 , $^3J^{(13)\text{C}-31\text{P}} = 12.5$ Hz), 186.7 (t, C_1 , $^2J^{(13)\text{C}-31\text{P}} = 36.3$ Hz). $^{31}\text{P}\{\text{H}\}$ NMR (121.49 MHz, C_6D_6): $\delta = 37.8$ ($J^{(31)\text{P}-117/119\text{Sn}} = 113$ /119 Hz). ^{31}P MAS NMR (161.98 MHz): $\delta = 34.4$, 33.2. $^{119}\text{Sn}\{\text{H}\}$ NMR (111.92 MHz, C_6D_6): $\delta = -99$ ($J^{(119)\text{Sn}-31\text{P}} = 119$ Hz). $^{119}\text{Sn}\{\text{H}\}$ MAS NMR (149.21 MHz): $\delta = -96$. Mössbauer spectroscopy: I.S. 2.93 mm·s⁻¹, Q.S. 3.30 mm·s⁻¹. Elemental analysis: $\text{C}_{22}\text{H}_{39}\text{ClO}_6\text{P}_2\text{Sn}$ (615.65 g·mol⁻¹); C 42.8 (calcd. 42.92); H 6.3 (6.39) %.

[2,6-Bis(diisopropoxyphosphonyl)-4-tert-butyl]phenyl}tin(II) bromide, [4-tBu-2,6-[P(O)(O-iPr)₂]₂C₆H₂]SnBr (4): A 0.75 M solution (*n*-hexane/ethyl ether: 1/0.8) of lithium diisopropyl amide (36 mL, 27.5 mmol) was added dropwise within 20 min to a solution of 4-tBu-2,6-[P(O)(O-iPr)₂]₂C₆H₃ (10.3 g, 22.2 mmol) in THF (80 mL). After stirring the reaction mixture for 7 h at -40 °C, SnBr₂ (4.7 g, 24.8 mmol) was added in small portions within 30 min at -30 °C. The reaction mixture was allowed to warm to room temperature overnight. After removing of the solvents in vacuo the residue was extracted with hot *n*-hexane (3 × 100 mL) to give 8.9 g (61 %) of compound 4 as pale yellow crystals, mp. 111 °C that were suitable for X-ray diffraction analysis. ^1H NMR (300.13 MHz, C_6D_6): $\delta = 0.05$ (d, 12 H, $\text{CH}(\text{CH}_3)(\text{CH}_3)'$, $^3J^{(1)\text{H}-1\text{H}} = 6.2$ Hz), 1.17 (s, 9 H, $\text{C}(\text{CH}_3)_3$), 1.30 (d, 12 H, $\text{CH}(\text{CH}_3)(\text{CH}_3)'$, $^3J^{(1)\text{H}-1\text{H}} = 5.9$ Hz), 4.92 (m, 4 H, $\text{CH}(\text{CH}_3)_2$, $^3J^{(1)\text{H}-1\text{H}} = 6.0$, $^3J^{(1)\text{H}-31\text{P}} = 7.5$ Hz), 8.10 (d, 2 H, $\text{H}_3/5$, $^3J^{(31)\text{P}-1\text{H}} = 13.5$ Hz). $^{13}\text{C}\{\text{H}\}$ NMR (75.47 MHz, C_6D_6): $\delta = 23.5$ (d, $\text{CH}(\text{CH}_3)(\text{CH}_3)'$, $J^{(13)\text{C}-31\text{P}} = 4.8$ Hz), 23.8 (d, $\text{CH}(\text{CH}_3)(\text{CH}_3)'$, $J^{(13)\text{C}-31\text{P}} = 3.9$ Hz), 30.7 (s, $\text{C}(\text{CH}_3)_3$), 34.4 (s, $\text{C}(\text{CH}_3)_3$), 72.1 (d, $\text{CH}(\text{CH}_3)_2$, $J^{(13)\text{C}-31\text{P}} = 4.9$ Hz), 131.6 (dd, C_3/C_5 , $^2J^{(13)\text{C}-31\text{P}} = 17.0$, $^4J^{(13)\text{C}-31\text{P}} = 4.4$ Hz), 150.0 (t, C_4 , $^3J^{(13)\text{C}-31\text{P}} = 12.0$ Hz), 174.2 (dd, C_2/C_6 , $^1J^{(13)\text{C}-31\text{P}} = 54.1$, $^3J^{(13)\text{C}-31\text{P}} = 4.7$ Hz), 184.6 (t, C_1 , $^2J^{(13)\text{C}-31\text{P}} = 35.3$ Hz). $^{31}\text{P}\{\text{H}\}$ NMR (121.49 MHz, C_6D_6): $\delta = 37.6$ ($J^{(31)\text{P}-117/119\text{Sn}} = 114/118$ Hz). $^{119}\text{Sn}\{\text{H}\}$ NMR (111.92 MHz, C_6D_6): $\delta = -69$ ($J^{(31)\text{P}-119\text{Sn}} = 118$ Hz). Mössbauer spectroscopy: I.S. 3.02 mm·s⁻¹, Q.S. 3.32 mm·s⁻¹. Elemental analysis: $\text{C}_{22}\text{H}_{39}\text{BrO}_6\text{P}_2\text{Sn}$ (660.10 g·mol⁻¹); C 39.9 (calcd. 40.03); H 5.7 (5.96) %.

{[2,6-Bis(diisopropoxyphosphonyl)-4-tert-butyl]phenyl}tin(II) iodide, [4-tBu-2,6-[P(O)(O-iPr)₂]₂C₆H₂]SnI (5): A 0.75 M solution (*n*-hexane/diethyl ether: 1/0.8) of lithium diisopropyl amide (27.5 mmol, 36 mL) was added dropwise within 20 min to a solution of 4-tBu-2,6-[P(O)(O-iPr)₂]₂C₆H₃ (10.3 g, 22.2 mmol) in THF (80 mL). After stirring the reaction mixture for 7 h at -40 °C, SnI₂ (4.7 g, 24.8 mmol) was added in small portions within 30 min at -30 °C. The reaction mixture was allowed to warm to room temperature overnight. After the solvents had been removed in vacuo, the residue was extracted with hot *n*-hexane (3 × 100 mL) to afford 8.3 g (53 %) of compound 5 as deep yellow crystals of mp. 138 °C that were suitable for X-ray diffraction analysis. ^1H NMR (300.13 MHz, C_6D_6): $\delta = 0.96$ (d, 12 H, $\text{CH}(\text{CH}_3)(\text{CH}_3)'$, $^3J^{(1)\text{H}-1\text{H}} = 6.2$ Hz), 1.05 (s, 9 H, $\text{C}(\text{CH}_3)_3$), 1.19 (d, 12 H, $\text{CH}(\text{CH}_3)(\text{CH}_3)'$, $^3J^{(1)\text{H}-1\text{H}} = 6.0$ Hz), 4.83 (m, 4 H, $\text{CH}(\text{CH}_3)_2$, $^3J^{(1)\text{H}-1\text{H}} = 6.0$, $^3J^{(31)\text{P}-1\text{H}} = 7.5$ Hz), 7.96 (d, 2 H, $\text{H}_3/5$, $^3J^{(31)\text{P}-1\text{H}} = 13.4$ Hz). $^{13}\text{C}\{\text{H}\}$ NMR (75.47 MHz, C_6D_6): $\delta = 23.5$ (d, $\text{CH}(\text{CH}_3)(\text{CH}_3)'$, $J^{(13)\text{C}-31\text{P}} = 4.8$ Hz), 23.8 (d, $\text{CH}(\text{CH}_3)(\text{CH}_3)'$, $J^{(13)\text{C}-31\text{P}} = 3.9$ Hz), 30.7 (s, $\text{C}(\text{CH}_3)_3$), 34.4 (s, $\text{C}(\text{CH}_3)_3$), 72.1 (d, $\text{CH}(\text{CH}_3)_2$, $^2J^{(13)\text{C}-31\text{P}} = 4.9$ Hz), 131.6 (dd, C_3/C_5 , $^2J^{(13)\text{C}-31\text{P}} = 16.4$, $^4J^{(13)\text{C}-31\text{P}} = 4.2$ Hz), 132.8 (dd, C_2/C_6 , $^1J^{(13)\text{C}-31\text{P}} = 192.7$, $^3J^{(13)\text{C}-31\text{P}} = 23.7$ Hz), 151.1 (t, C_4 , $^3J^{(13)\text{C}-31\text{P}} = 12.2$ Hz), 182.6 (t, C_1 , $^2J^{(13)\text{C}-31\text{P}} = 35.5$ Hz). $^{31}\text{P}\{\text{H}\}$ NMR (121.49 MHz, C_6D_6): $\delta = 36.9$.

($J^{(31)\text{P}-117/119\text{Sn}} = 112/117$ Hz). $^{119}\text{Sn}\{\text{H}\}$ NMR (111.92 MHz, C_6D_6): $\delta = -22$ ($J^{(31)\text{P}-119\text{Sn}} = 117$ Hz). Mössbauer spectroscopy: I.S. 3.07 mm·s⁻¹, Q.S. 3.23 mm·s⁻¹. Elemental analysis: $\text{C}_{22}\text{H}_{39}\text{IO}_6\text{P}_2\text{Sn}$ (707.10 g·mol⁻¹); C 37.1 (calcd. 37.37); H 5.9 (5.56) %.

{[2,6-Bis(diisopropoxyphosphonyl)-4-tert-butyl]phenyl}tin(II) thionaphthalene, [4-tBu-2,6-{P(O)(O-iPr)₂}₂C₆H₂]SnSPh (6): Under magnetically stirring and at room temperature, sodium thiophenolate, Ph₂SnA, (0.055 g, 0.42 mmol) was added to a solution of {4-tBu-2,6-[P(O)(O-iPr)₂]₂C₆H₂}SnCl (3) (0.251 g, 0.41 mmol) in THF (20 mL). After the reaction mixture had been stirred for 24 h, the precipitate of sodium chloride was filtered. The solvent of the filtrate was removed in vacuo to give a solid residue. The latter was recrystallized from toluene (10 mL) to afford 187 mg (66 %) of compound 6 as colorless crystals (m.p. 124–126 °C). ^1H NMR (400.13 MHz, $[\text{D}_8]$ toluene): $\delta = 0.95$ (d, 6 H, $\text{CH}(\text{CH}_3)(\text{CH}_3)'$, $^3J^{(1)\text{H}-1\text{H}} = 6.3$ Hz), 1.05 (d, 6 H, $\text{CH}(\text{CH}_3)(\text{CH}_3)'$, $^3J^{(1)\text{H}-1\text{H}} = 6.0$ Hz), 1.15 (s, 9 H, $\text{C}(\text{CH}_3)_3$), 1.16 (d, 6 H, $\text{CH}(\text{CH}_3)(\text{CH}_3)'$, $^3J^{(1)\text{H}-1\text{H}} = 6.0$ Hz), 1.33 (d, 6 H, $\text{CH}(\text{CH}_3)(\text{CH}_3)'$, $^3J^{(1)\text{H}-1\text{H}} = 6.0$ Hz), 4.44–4.49 (unresolved multiplet, 2 H, $\text{CH}(\text{CH}_3)_2$), 5.20–5.25 (unresolved multiplet, 2 H, $\text{CH}(\text{CH}_3)_2$), 6.94–7.14 (complex pattern, 3 H, CH_{SPh}), 7.95–7.99 (complex pattern, 4 H, $\text{CH}_{\text{SPh}} + \text{CH}_{\text{aryl3/5}}$). $^{13}\text{C}\{\text{H}\}$ NMR (100.63 MHz, $[\text{D}_8]$ toluene): $\delta = 23.2$ –23.8 (complex pattern, $\text{CH}(\text{CH}_3)_2$), 30.6 (s, $\text{C}(\text{CH}_3)_3$), 34.2 (s, $\text{C}(\text{CH}_3)_3$), 71.2 (d, $\text{CH}(\text{CH}_3)_2$, $J^{(13)\text{C}-31\text{P}} = 5.3$ Hz), 71.8 (d, $\text{CH}(\text{CH}_3)_2$, $J^{(13)\text{C}-31\text{P}} = 3.9$ Hz), 127.9 (s, $\text{C}_{\text{SPh}-meta}$), 128.7 (s, $\text{C}_{\text{SPh}-ortho}$), 131.2 (dd, C_3/C_5 , $^2J^{(13)\text{C}-31\text{P}} = 16.5$, $^4J^{(13)\text{C}-31\text{P}} = 4.4$ Hz), 133.1 (s, $\text{C}_{\text{SPh}-para}$), 133.5 (dd, C_2/C_6 , $^1J^{(13)\text{C}-31\text{P}} = 192.4$, $^3J^{(13)\text{C}-31\text{P}} = 23.8$ Hz), 142.9 (s, $\text{C}_{\text{SPh}-ipso}$), 150.2 (t, C_4 , $^3J^{(13)\text{C}-31\text{P}} = 12.6$ Hz), 182.9 (t, C_1 , $^2J^{(13)\text{C}-31\text{P}} = 35.2$ Hz). $^{31}\text{P}\{\text{H}\}$ NMR (161.98 MHz, $[\text{D}_8]$ toluene): $\delta = 35.3$ ($J^{(31)\text{P}-119/117\text{Sn}} = 97$ Hz). $^{119}\text{Sn}\{\text{H}\}$ NMR (149.21 MHz, $[\text{D}_8]$ toluene): $\delta = -2$ ($J^{(31)\text{P}-119\text{Sn}} = 98$ Hz). IR (KBr): $\tilde{\nu}(\text{P=O}) = 1193$ cm⁻¹, 1180 cm⁻¹. No elemental analysis was performed.

[2,6-Bis(diisopropoxyphosphonyl)-4-tert-butyl]phenyl}lead(II) chloride, [4-tBu-2,6-{P(O)(O-iPr)₂}₂C₆H₂]PbCl (7): At -60 °C, a 0.75 M solution (36 mL, *n*-hexane/diethyl ether: 1/0.8) of lithium diisopropyl amide (27.5 mmol) was added dropwise over a period of 20 min to a solution of 4-tBu-2,6-[P(O)(O-iPr)₂]₂C₆H₃ (10.3 g, 22.2 mmol) in THF (80 mL). After stirring the yellow reaction mixture for 7 h at -40 °C, within 30 min, lead dichloride, PbCl₂ (6.9 g, 24.8 mmol) was added in small portions. The reaction mixture was stirred for additional 12 h during which it warmed to room temperature. After evaporating all volatiles in vacuo the residue was extracted three times with hot *n*-hexane (3 × 70 mL). The extracts were combined and the solvents evaporated in vacuo to give a solid material. This was recrystallized from hot *n*-hexane to afford 3.20 g (20 %) of compound 7 as colorless crystals of mp. 159 °C (decomposition). ^1H NMR (300.13 MHz, C_6D_6): $\delta = 1.06$ (d, 6 H, $\text{CH}(\text{CH}_3)(\text{CH}_3)'$, $^3J^{(1)\text{H}-1\text{H}} = 6.0$ Hz), 1.25 (d, 6 H, $\text{CH}(\text{CH}_3)(\text{CH}_3)'$, $^3J^{(1)\text{H}-1\text{H}} = 6.0$ Hz), 1.32 (s, 9 H, $\text{C}(\text{CH}_3)_3$), 1.35 (d, 6 H, $\text{CH}(\text{CH}_3)(\text{CH}_3)'$, $^3J^{(1)\text{H}-1\text{H}} = 6.0$ Hz), 1.41 (d, 6 H, $\text{CH}(\text{CH}_3)(\text{CH}_3)'$, $^3J^{(1)\text{H}-1\text{H}} = 6.0$ Hz), 4.66 (m, 2 H, $\text{CH}(\text{CH}_3)_2$, $^3J^{(1)\text{H}-1\text{H}} = 6.1$, $^3J^{(31)\text{P}-1\text{H}} = 7.3$ Hz), 4.86 (m, 2 H, $\text{CH}(\text{CH}_3)_2$, $^3J^{(1)\text{H}-1\text{H}} = 6.1$, $^3J^{(31)\text{P}-1\text{H}} = 7.3$ Hz), 8.06 (AXX', 2 H, CH_{aryl} , $^3J^{(31)\text{P}-1\text{H}} = 13.0$ Hz). $^{31}\text{P}\{\text{H}\}$ NMR (121.49 MHz, C_6D_6): $\delta = 50.5$ ($J^{(31)\text{P}-207\text{Pb}} = 125$ Hz). Elemental analysis: $\text{C}_{22}\text{H}_{39}\text{ClO}_6\text{P}_2\text{Pb}$ (705.14); C 36.9 (calcd. 37.47); H 5.4 (5.57) %.

{[2,6-Bis(diisopropoxyphosphonyl)-4-tert-butyl]phenyl}tin(II) chloride tungsten pentacarbonyl, {[2,6-{P(O)(O-iPr)₂}₂-4-tBu]C₆H₂}SnCl[Cr(CO)₅] (8): A solution of the organostannylene {4-tBu-2,6-[P(O)(O-iPr)₂]₂C₆H₂}SnCl (3) (1.55 g, 2.5 mmol) and chromium hexacarbonyl, Cr(CO)₆ (0.55 g, 2.5 mmol) in THF (250 mL) was irradiated

ated with UV light (Hg high pressure lamp, 150 W) until the formation of carbon monoxide gas stopped. After removing the solvent in vacuo the yellow-green residue was extracted with toluene (40 mL). The toluene solution was concentrated in vacuo to one third of its volume and stored at -30 °C to give 1.71 g (85 %) of compound **8**, as its toluene solvate 8·0.5 C₇H₈, as yellow crystals of m.p. 139–141 °C. ¹H NMR (400.13 MHz, C₆D₆): δ = 0.94 (d, 6 H, CH(CH₃)(CH₃)₃), ³J(H-H) = 6.0 Hz), 1.10 (s, 15 H, C(CH₃)₃ + CH(CH₃)₂, v_{1/2} = 12 Hz), 1.24 (d, 6 H, CH(CH₃)(CH₃)₃), ³J(H-H) = 7.5 Hz), 1.26 (d, 6 H, CH(CH₃)(CH₃)₃), ³J(H-H) = 6.7 Hz), 4.74–4.96 (complex pattern, 4 H, CH(CH₃)₂), 8.06 (d, CH_{aryl}, ³J(H-³¹P) = 13.3 Hz). ¹³C{¹H} NMR (100.63 MHz, C₆D₆): δ = 21.0 (complex pattern, CH(CH₃)(CH₃)₃), 21.3 (complex pattern, CH(CH₃)(CH₃)₃), 21.5 (complex pattern, CH(CH₃)(CH₃)₃), 30.4 (s, C(CH₃)₃), 34.6 (s, C(CH₃)₃), 73.6–73.8 (complex pattern, CH(CH₃)₂), 131.8 (dd, C_{3/5}, ²J(¹³C-³¹P) = 14.6, ⁴J(¹³C-³¹P) = 4.8 Hz), 131.8 (dd, C_{2/6}, ¹J(¹³C-³¹P) = 188.1, ³J(¹³C-³¹P) = 19.9 Hz), 153.7 (t, C_{4/aryl}, ³J(¹³C-³¹P) = 11.2 Hz), 171.7 (t, C₁, ²J(¹³C-³¹P) = 25.8 Hz), 219.4 (s, CO_{cis}, ²J(¹³C-¹¹⁹Sn) = 129.3 Hz), 225.7 (s, CO_{trans}). ³¹P{¹H} NMR (161.98 MHz, C₆D₆): δ = 30.4 (¹J(³¹P-¹¹⁷¹¹⁹Sn) = 178 Hz). ¹¹⁹Sn{¹H} NMR (149.21 MHz, C₆D₆): δ = 127.9 (J(¹¹⁹Sn-³¹P) = 182 Hz). IR (Nujol): ν(P=O) = 1182 cm⁻¹, 1155 cm⁻¹; ν(CO) = 1932 cm⁻¹, 2051 cm⁻¹. Mössbauer spectroscopy: IS = 2.01 mm·s⁻¹, QS = 3.50 mm·s⁻¹. Elemental analysis: C₂₇H₃₉P₂O₁₁SnCrCl·0.5 C₇H₈ (853.84 g·mol⁻¹); C 42.7 (calcd. 42.90), H 5.0 (5.08 %).

Supporting Information (see footnote on the first page of this article): Molecular structure of **4** (Figure S1), calculated structure (BP86/def2-TZVP) of the hypothetical compound *p-t*-BuC₆H₄SnI (Figure S2) and molecular orbital interaction diagram of compound **3** (Figure S3).

Acknowledgement

We thank Dr. G. Bradtmöller for recording the ³¹P and ¹¹⁹Sn MAS NMR spectra and Professor B. Costisella for performing the NOE experiments. Mrs. Sylvia Marzian is acknowledged for recording the electrospray ionization mass spectra.

References

- This work contains parts of the PhD theses of Markus Henn (TU Dortmund 2004 and Vajk Deák (TU Dortmund 2010). Parts of it were first presented at the XVth FECHEM Conference on Organometallic Chemistry, University of Zürich, 10th to 15th August 2003, Book of Abstracts OP38, and at the 11th and 12th International Conferences on the Coordination and Organometallic Chemistry of Germanium, Tin, and Lead (IC-COC-GTL-11), Santa Fe (New Mexico, USA) 27th June to 2nd July 2004, Book of Abstracts O54, respectively ICCOC-GTL-12, Galway (Ireland), July 9–13, 2007, Book of Abstracts O4.
- [1] a) L. M. Engelhardt, B. S. Jolly, M. F. Lappert, C. L. Raston, A. H. White, *J. Chem. Soc., Chem. Commun.* **1988**, 336–338; b) J. T. B. H. Jastrzebski, P. A. van der Schaaf, J. Boersma, G. van Koten, *Organometallics* **1989**, 8, 1373–1375; c) K. Jurkschat, C. Klaus, M. Dargatz, A. Tzsachach, J. Meunier-Piret, B. Mahieu, *Z. Anorg. Allg. Chem.* **1989**, 577, 122–134; d) B. S. Jolly, M. F. Lappert, L. M. Engelhardt, A. H. White, C. L. Raston, *J. Chem. Soc., Dalton Trans.* **1993**, 2653–2663; e) A. J. Edwards, M. A. Paver, P. R. Ralby, M.-A. Rennie, C. A. Russel, D. S. Wright, *J. Chem. Soc., Dalton Trans.* **1995**, 1587–1591; f) R. S. Simons, L. H. Pu, M. M. Olmstead, P. P. Power, *Organometallics* **1997**, 16, 1920–1925; g) C. Drost, P. B. Hitchcock, M. F. Lappert, L. J. M. Pierssens, *Chem. Commun.* **1997**, 1141–1142; h) C. Drost, B. Gehrhus, P. B. Hitchcock, M. F. Lappert, *Chem. Commun.* **1997**, 1845–1846; i) C. J. Cardin, D. J. Cardin, S. P. Constantine, M. G. B. Drew, H. Rashid, M. A. Convery, D. Fenske, *J. Chem. Soc., Dalton Trans.* **1998**, 2749–2756; j) W. P. Leung, W.-H. Kwok, F. Xue, T. C. W. Mak, *J. Am. Chem. Soc.* **1997**, 119, 1145–1146; k) C. Eaborn, P. B. Hitchcock, J. D. Smith, S. E. Soezerli, *Organometallics* **1997**, 16, 5653–5658; l) L. H. Pu, M. M. Olmstead, P. P. Power, B. Schiemenz, *Organometallics* **1998**, 17, 5602–5606; m) M. M. Olmstead, R. S. Simons, P. P. Power, *J. Am. Chem. Soc.* **1997**, 119, 11705–11706; n) A. A. Barney, A. F. Heyduk, D. G. Nocera, *Chem. Commun.* **1999**, 2379–2380; o) M. Mehring, C. Löw, M. Schürmann, F. Uhlig, K. Jurkschat, B. Mahieu, *Organometallics* **2000**, 19, 4613–4623; p) B. E. Eichler, L. H. Pu, M. Stender, P. P. Power, *Polyhedron* **2001**, 20, 551–556; q) S. S. Al-Juaid, A. G. Avent, C. Eaborn, M. S. Hill, P. B. Hitchcock, D. J. Patel, J. D. Smith, *Organometallics* **2001**, 20, 1223–1229; r) Y. Ding, H. W. Roesky, M. Noltemeyer, H.-G. Schmidt, *Organometallics* **2001**, 20, 1190–1194; s) A. Jana, H. W. Roesky, C. Schulzke, A. Döring, T. Beck, A. Pal, R. Herbst-Irmer, *Inorg. Chem.* **2009**, 48, 193–197; t) M. Weidenbruch, U. Grobecker, W. Saak, E.-M. Peters, K. Peters, *Organometallics* **1998**, 17, 5206–5208; u) S. Benet, C. J. Cardin, D. J. Cardin, S. P. Constantine, P. Heath, R. Haroon, S. Teixeira, J. H. Thorpe, A. K. Todd, *Organometallics* **1999**, 18, 389–398; v) Y. Mizuhata, T. Sasamori, N. Tokitoh, *Chem. Rev.* **2009**, 109, 3479–3511.
 - [2] J. T. B. H. Jastrzebski, P. A. van der Schaaf, J. Boersma, G. van Koten, M. de Wit, Y. Wang, D. Heijdenrijk, C. H. Stam, *J. Organomet. Chem.* **1991**, 407, 301–311.
 - [3] a) P. P. Power, *Organometallics* **2007**, 26, 4362–4372, and references cited therein; b) E. Rivard, P. P. Power, *Inorg. Chem.* **2007**, 46, 10047–10064; c) E. Rivard, P. P. Power, Dalton Discussion 11, *The Renaissance of Main Group Chemistry*, University of California, Berkeley, USA, June 23–25, **2008**; Perspective K1; d) R. Jambor, B. Kasna, K. N. Kirschner, M. Schürmann, K. Jurkschat, *Angew. Chem. Int. Ed.* **2008**, 47, 1650–1653.
 - [4] a) A. C. Filippou, A. I. Philippopoulos, G. Schnakenburg, *Organometallics* **2003**, 22, 3339–3341; b) A. C. Filippou, P. Portius, A. I. Philippopoulos, H. Rohde, *Angew. Chem.* **2003**, 115, 461–464; *Angew. Chem. Int. Ed.* **2003**, 42, 445–447.
 - [5] B. Eichler, A. D. Phillips, S. T. Haubrich, B. V. Mork, P. P. Power, *Organometallics* **2002**, 21, 5622–5627.
 - [6] E. Rivard, J. Steiner, J. C. Fettinger, J. R. Giuliani, M. P. Augustine, P. P. Power, *Chem. Commun.* **2007**, 4919–4921.
 - [7] P. B. Hitchcock, M. F. Lappert, A. V. Protchenko, G. H. Uiterweerd, *Dalton Trans.* **2009**, 353–361.
 - [8] W.-P. Leung, W.-H. Kwok, Z.-Y. Zhou, T. C. W. Mak, *Organometallics* **2003**, 22, 1751–1755.
 - [9] C. Stanciu, A. F. Richards, P. P. Power, *J. Am. Chem. Soc.* **2004**, 126, 4106–4107.
 - [10] a) J. T. B. H. Jastrzebski, G. van Koten, *Adv. Organomet. Chem.* **1993**, 35, 241–294; b) J. T. B. H. Jastrzebski, D. M. Grove, J. Boersma, G. van Koten, J.-M. Ernsting, *Magn. Reson. Chem.* **1991**, 29, S25–S30.
 - [11] a) K. Dannappel, R. Nienhaus, M. Schürmann, B. Costisella, K. Jurkschat, *Z. Anorg. Allg. Chem.* **2009**, 635, 2126–2134; b) V. Deák, M. Schürmann, K. Jurkschat, *Z. Anorg. Allg. Chem.* **2009**, 635, 1380–1383; c) M. Henn, M. Schürmann, B. Mahieu, P. Zanotto, A. Cinquantini, K. Jurkschat, *J. Organomet. Chem.* **2006**, 691, 1560–1572; d) K. Peveling, K. Dannappel, M. Schürmann, B. Costisella, K. Jurkschat, *Organometallics* **2006**, 25, 368–374; e) K. Dannappel, M. Schürmann, B. Costisella, K. Jurkschat, *Organometallics* **2005**, 24, 1031–1034; f) K. Peveling, M. Henn, C. Löw, M. Mehring, M. Schürmann, B. Costisella, K. Jurkschat, *Organometallics* **2004**, 23, 1501–1508; g) K. Jurkschat, K. Peveling, M. Schürmann, *Eur. J. Inorg. Chem.* **2003**, 3563–3571; h) M. Henn, K. Jurkschat, R. Ludwig, M. Mehring, K. Peveling, M.

- Schürmann, *Z. Anorg. Allg. Chem.* **2002**, *628*, 2940–2947; i) K. Peveling, M. Schürmann, K. Jurkschat, *Z. Anorg. Allg. Chem.* **2002**, *628*, 2435–2442; j) K. Peveling, M. Schürmann, R. Ludwig, K. Jurkschat, *Organometallics* **2001**, *20*, 4654–4663; k) M. Mehrling, I. Vrasidas, D. Horn, M. Schürmann, K. Jurkschat, *Organometallics* **2001**, *20*, 4647–4653; l) K. Peveling, M. Schürmann, K. Jurkschat, *Main Group Met. Chem.* **2001**, *24*, 251–252; m) M. Mehrling, C. Löw, M. Schürmann, K. Jurkschat, *Eur. J. Inorg. Chem.* **1999**, 887–898; n) M. Mehrling, K. Jurkschat, M. Schürmann, *Main Group Met. Chem.* **1998**, *21*, 635–641; o) M. Mehrling, M. Schürmann, K. Jurkschat, *Organometallics* **1998**, *17*, 1227–1236.
- [12] J. E. Huheey, E. A. Keiter, R. L. Keiter, *Anorganische Chemie: Prinzipien von Struktur und Reaktivität*, Walter de Gruyter, Berlin New York **1995**, p. 335.
- [13] a) M. Henn, K. Jurkschat, D. Mansfeld, M. Mehrling, M. Schürmann, *J. Mol. Struct.* **2004**, *697*, 213–220; b) I. V. Alabugin, M. Manoharan, S. Scott Peabody, F. Weinhold, *J. Am. Chem. Soc.* **2003**, *125*, 5973–5987; c) M. Doskocz, R. Gancarz, *Phosphorus Sulfur Silicon Relat. Elem.* **2009**, *184*, 1363–1373.
- [14] U. Lay, H. Pritzkow, H. Grützmacher, *J. Chem. Soc., Chem. Commun.* **1992**, 260–262.
- [15] a) V. A. Lagunov, V. I. Polocenko, *Sov. Phys.-Solid State* **1973**, *15*, 1210; b) N. Mishima, M. Idogaki, H. Negita, *Shimane Daigaku Bunrigakubu Kiyo Rigaka Hen* **1974**, *7*, 73–77; c) J. Silver, C. A. Mackay, J. D. Donaldson, *J. Mater. Sci.* **1976**, *11*, 836–842.
- [16] P. A. W. Dean, J. J. Vittal, N. C. Payne, *Can. J. Chem.* **1985**, *63*, 394–400.
- [17] a) G. Barone, T. G. Hibbert, M. F. Mahon, K. C. Molloy, I. P. Parkin, L. S. Price, I. Silaghi-Dumitrescu, *J. Chem. Soc., Dalton Trans.* **2001**, 3435–3445; b) P. B. Hitchcock, J. Hu, M. F. Lap-
pert, J. R. Severn, *Dalton Trans.* **2004**, 4193–4201; c) J. Beckmann, S. Heitz, M. Hesse, *Inorg. Chem.* **2007**, *46*, 3275–3282; d) J. Beckmann, J. Bolsinger, A. Duthie, *Chem. Eur. J.* **2010**, ##in press, DOI: 10.1002/chem.201002371.
- [18] G. M. Sheldrick, *Acta Crystallogr., Sect. A* **1990**, *46*, 467–473.
- [19] G. M. Sheldrick, University of Göttingen, **1997**.
- [20] *International Tables for Crystallography*, Vol. C. Dordrecht: Kluwer Academic Publishers, **1992**.
- [21] G. M. Sheldrick, *SHELXTL*, Release 5.1, Software Reference Manual, Bruker AXS, Inc., Madison, Wisconsin, USA, **1997**.
- [22] a) *TURBOMOLE V6.1*, University of Karlsruhe and Forschungszentrum Karlsruhe GmbH, Turbomole GmbH (since 2007), **2009**; b) K. Eichhorn, O. Treutler, H. Öhm, M. Häser, R. Ahlrichs, *Chem. Phys. Lett.* **1995**, *242*, 652–660.
- [23] A. D. Becke, *J. Chem. Phys.* **1986**, *84*, 4524–4529; A. D. Becke, *J. Chem. Phys.* **1988**, *88*, 1053–1062.
- [24] A. D. Becke, *Phys. Rev. A* **1988**, *38*, 3098–3100.
- [25] J. P. Perdew, *Phys. Rev. B* **1986**, *33*, 8822–8824; J. P. Perdew, *Phys. Rev. B* **1986**, *34*, 7406–7406.
- [26] R. Ahlrichs, M. Bär, M. Häser, H. Horn, C. Kölmel, *Chem. Phys. Lett.* **1989**, *162*, 165–169.
- [27] M. Häser, R. Ahlrichs, *J. Comput. Chem.* **1989**, *10*, 104–111.
- [28] B. I. Dunlap, J. W. D. Connolly, J. R. Sabin, *J. Chem. Phys.* **1979**, *71*, 3396–3402.
- [29] S. Grimme, *J. Comput. Chem.* **2006**, *27*, 1787–1799.
- [30] F. Weigend, M. Häser, H. Patzelt, R. Ahlrichs, *Chem. Phys. Lett.* **1998**, *294*, 143–152.

Received: October 26, 2010

Published Online: December 29, 2010